COMPLETE AND INCOMPLETE FUSION REACTIONS IN $^{16}O + ^{93}Nb$ SYSTEMS AT VARIOUS PROJECTILE ENERGIES

By

Desalegn Ketema

SUBMITTED IN PARTIAL FULFILLMENT OF THE
REQUIREMENTS FOR THE DEGREE OF
MASTER OF SCIENCE IN PHYSICS
AT
ADDIS ABABA UNIVERSITY
ADDIS ABABA, ETHIOPIA
JUNE 2013

ADDIS ABABA UNIVERSITY

DEPARTMENT OF

PHYSICS

The undersigned hereby certify that they have read and recommend to the school of Graduate Studies for acceptance a thesis entitled "COMPLETE AND INCOMPLETE FUSION REACTIONS IN $^{16}O +^{93} Nb$ SYSTEMS AT VARIOUS PROJECTILE ENERGIES "by Desalegn Ketema in partial fulfillement of the requirements for the degree of MASTERS OF SCIENCE IN PHYSICS.

June 2013

Supervisor: _____
Prof.A.K.CHAUBEY

Examiners: _____
DR. TILAHUN TESFAYE

_____
Prof. SINGH K.P.

ADDIS ABABA UNIVERSITY

Date: **June 2013**

Author: **Desalegn Ketema**

Title: **COMPLETE AND INCOMPLETE FUSION REACTIONS IN $^{16}O + ^{93}Nb$ SYSTEMS AT VARIOUS PROJECTILE ENERGIES**

Department: **Physics**

Degree: **M.Sc.** Convocation: Year: **2013**

Permission is herewith granted to Addis Ababa University to circulate and to have copied for non-commercial purposes, at its discretion, the above title upon the request of individuals or institutions.

Signature of Author

Table of Contents

List of Tables

List of Figures

Acknowledgements

Above all, I would like to thank the almighty; God, for letting me accomplish this stage. I am deeply indebted to professor A.K.chaubey, my Advisor, for his many suggestions and constant support and friendly approach during this research. His tireless follow up and his consistent support will be in my memory forever.
My strongest thank is addressed to my Family especially to my Mother Bekelech Dadi and my intimate Friends. Finally I would like to thank Addis Ababa University(department of physics) for the financial support provided and for extending facilities for carrying out this thesis.

Abstract

In this work Complete and Incomplete fusion in the reaction $^{16}O +^{93} Nb$ System in the energy range of 70-100 MeV have been Studied. Excitation function(EFs) of Various reaction products populated via CF and/or ICF Of ^{16}O projectile with ^{93}Nb target were studied at various projectile energies.From this Excitation functions study the complete and incomplete fusion reactions in light(medium) target nucleus could be studide.It has been obserbed that complete and incomplete fusion reactions play important role in heavy ion reactions at these energies.The experimental excitation functions have been compared with theoretical values calculated using computer code PACE4.

The experimentally studied production cross-sections for non-α emitting channels were found to be in good agreement with theoretical predictions which may be attributed to the complete fusion (CF) processes at these energies,In general. However in case of α-emitting channels, the experimental excitation functions exhibit a significant enhancement in the production cross-section, which may be credited to the incomplete fusion (ICF) reaction at these energies.An attempt was made to estimate the percentage of incomplete fusion fraction to get the relative importance of complete and incomplete fusion reactions.

Chapter 1

INTRODUCTION

For many years,the study of heavy ion induced reaction has been used as important tools to understand the reaction dynamics and the decay characteristics of excited compound nuclei at energies near and above the coulomb barrier(CB). in recent years, the study of heavy ion induced reactions has been become a topic of interest in nuclear physics, especially Complete Fusion(CF) and Incomplete Fusion(ICF) process [1, 2]. CF is the process in which the projectile completely fuses with the target, which leads to the formation of excited composite system. And then it de-excites by particle and/or γ-ray emission. Where as in case of ICF mechanism, the projectile breaks into two fragments, of which one will fuse with the target to form an excited composite system, which may decay via emission of light-particles and/or γ-rays, while the other fragment moves forward as spectator with same velocity as that of the projectile carrying a large part of the angular momentum and kinetic energy of the projectile.

The first evidence of ICF process was observed by Britt and Quinton [3]. The later study done by Inamura et al [4] gave more strength to illustrate the ICF reaction dynamics. Several theoretical models have been proposed to explain the ICF dynamics, for example, Sum- rule model of Wilczynski et al., Break up fusion model by Udagawa and Tamura, etc. Hence despite of the existence of so many models, a clear picture of the mechanism of ICF reactions is yet to emerge. There are certain aspects far from being completely

understood. As such, the study of competition between Complete Fusion (CF) and Incomplete Fusion (ICF) is still an open area of investigation in nuclear physics. Thus more and more experimental data is required to determine the optimum irradiation conditions for the production yield of various radioisotopes for better understanding of the phenomena of CF and ICF of heavy ion (HI) systems, formed in HI reactions. There are some observables, e.g.,excitation functions, recoil range distributions, angular distributions and spin distributions which are related to CF and ICF. The present work has been carried out with the aim to study more information about CF and ICF reaction in $^{16}O + {}^{93}Nb$ system at various projectile energies ranging from 70-100 MeV.

The most common features of ICF reaction are

i)the outgoing particles have forward peaked angular distribution and energy spectrum peaked at beam velocity[5].

ii)the recoil range distiribution of the heavy residues show a low range components suggesting incomplete momentem transfer.

Recently,it has been observed that ICF becomes more and more dominant as the projectile energy increases[6].it is known that CF reaction occurs where the angular momentum imparted to the system is less than or equal to l_{crit}[7].In sharp-cut approximation the probability of CF is assumed to be unity for l$\approx l_{crit}$ and expected to be zero for l $> l_{crit}$[8];while at relatively higher projectile energies and at finite values of impact parametere CF gradually gives way to ICF.

As mentioned above several dynamical models have been proposed to explain the mechanism of ICF reactions. The break-up fusion model of Tamura and Udagawa[9] explained ICF in terms of the break-up of the projectile in the nuclear force field of the target nucleus followed by fusion of one of the fragments with the target. The model uses distorted wave Born approximation to evaluate the shapes of the energy spectra and angular distributions of projectile like fragements but does not give absolute cross-sections,due to lack of information about the spectroscopic form factors of the continuum

states of the product nuclei. The sum rule model of Wilczynski et al.[10] assumes that the various ICF Channels are localized in the angular momentum space above the critical angular momentum for a complete fusion of the projectile and target to occur.The model gives cross-sections reaction products arising not only from ICF and quasi-elastic transfer reactions but also from CF Other dynamical models,like the Exciton model[11],the Hot spot model[12],the promptly Emitted particles model[13],and the Multistep Direct Reaction model[14] have been proposed to explain ICF dynamics.

In the present work measured EFs for reactions $^{93}Nb(^{16}O,3n)^{106}In$, $^{93}Nb(^{16}O,4n)^{105}In$, $^{93}Nb(^{16}O,P3n)^{105}Cd$,$^{93}Nb(^{16}O,p4n)^{104}Cd$, $^{93}Nb(^{16}O,\alpha)^{105}Ag$, $^{93}Nb(^{16}O,\alpha n)^{104}Ag$,$^{93}Nb(^{16}O,\alpha 2n)^{103}Ag$, $^{93}Nb(^{16}O,\alpha 3n)^{102}Ag$,$^{93}Nb(^{16}O,\alpha 4n)^{101}Ag$,$^{93}Nb(^{16}O,\alpha p3n)^{101}Pd$,$^{93}Nb(^{16}O,\alpha p4n)^{100}Pd$, $^{93}Nb(^{16}O,2\alpha n)^{100}Rh$,$^{93}Nb(^{16}O,2\alpha 2n)^{99}Rh$, $^{93}Nb(^{16}O,2\alpha 3n)^{98}Rh$ and $^{93}Nb(^{16}O,3\alpha n)^{96}Tc$ in the incident energy range $70-100MeV$ were taken from literature [15] and EFs have been compared with theoretical predictions based on PACE4 codes. In these thesis Expermentally Measured EFs were then compared with the production of the statistical model code Pace4 ,here the nuclear level density (NLD) is an important ingredient in the statistical model calculation of nuclear cross section and the analysis of the results have been discussed. Further, the dependence of ICF fraction with projectile energy has also been discussed and finally conclusions are drawn.

Chapter 2

THEORIES OF NUCLEAR REACTION

2.1 Description of nuclear reaction

Nuclear reaction is a large subject by itself.in this paper we will see an Overview of some of the more important points. One important field of research to understand nuclear properties is study of nuclear reactions. Most of our knowledge of the atomic reaction has been based on the results of collision experiments between a target and various projectiles like electron , nucleon ,heavy nuclei, etc. Nuclear reaction is a process that occurs when two nucleons or combinations of nucleons(heavy ion)comes close together so that they are in the nuclear force range an interaction take place in which there may be transfer of energy,momentem and transfer of matter(nucleons) such type of interactions termed as nuclear reactions. Most of nuclear reactions are produced by exposing different materials to abeam of accelarated nuclear particles. for nuclear reactions to occur the energy must be high enough to overcome the natural repulsion between the protons. This energy barrier is called the Coulomb barrier.If the energy is below the barrier,the reaction will bounce off each other. In General nuclear reaction is represented by

$$A + B \Longrightarrow C + D + Q \tag{2.1.1}$$

Where

A=is a projectile or bombarding particle

B=is target nucleus (at rest in the lab.system)

C=is residual nucleus or light reaction product

D=is emitted particles or heavy reaction product

Q=the energy released or absorbed

To shorten the notation a reaction of the type (2.1.1) is designated by:

$$B(A, D)C \tag{2.1.2}$$

There are different types of nuclear reactions. such as

✓Elastic Scattering

✓In-Elastic Scattering

✓Radiative Capture

✓Dis integration processes

✓Nuclear Fusion and Nuclear Fission

✓Stripping and Pick up reaction etc

∗Elastic Scattering:- The Projectile A after interaction is emitted with the same energy.the target nucleus B is also remains in the initial quantum mechanical state. In this type of interaction intering projectile and emitted particle are same,target nucleus and residual nucleus are also same. There is no appreciable energy loss so the systems remains in the same ground state no excitation,there is only that much energy loss which is required for the conservation of linear momentume.

∗In-Elastic scattering:-is the scattering in which there is energy loss of projectile.here the emitted particle is same as the initial projectile but its energy is reduced. some energy taken by target nucleus and it goes to excited state.

$a + A \longrightarrow A^* + a$ $(Decreased\ Energy)$

A is in excited state and when comes in ground states γ-rays are emitted.

$A^* \longrightarrow A + \gamma$

∗Radiative Capture:-The projectile is Captured by target nucleus and a new system is formed in the excited state. which will come down in the ground state by emitting γ-radiation.After Capture Of Projectile Only γ-radiation are Emitted.

Exampel

${}^1_0n + {}^{208}Pb \longrightarrow {}^{209}Pb^* \longrightarrow {}^{209}Pb + \gamma$

∗Dis integration processes:-This means when a projectile enters the target nucleus a new system is formed. This may decay to residual nucleus B and a particle b is emitted or this may decay to asystem C and a particle c is emitted. its decay is depending up on the energy of reaction product.

Example

$A + a \longrightarrow B + b$

$A + a \longrightarrow C + c$

∗Nuclear Fusion and Nuclear Fission reactions:-are also other types of nuclear reactions.In Fusion reaction there is a combination of two nuclei to form a more massive nucleus where as In Fission reactions there is spallation,the interactions in which heavy nucleus splits in to two medium nucleies.

2.2 Conservation laws and Energies in nuclear reactions

Nuclear reactions are subject of the conservation laws.These laws are the conservation of energy,total charge,mass number,momentum(linear and angular),spin,parity,baryon number,lepton number,etc.

In every type of nuclear reaction the total charge before the nuclear reaction is same as the total charge after the reaction. That is the total charge number is conserved. The

other is conservation of mass number; according to this law the total number of nucleons before and after the collision must be same. This result together with the law of conservation of charge implies that the total number of nucleons is also conserved. The total angular momentum J before the reaction is the vector sum of the spin angular momenta (I_1,I_2) and the relative orbital angular momenta(l) i.e $J = I_1 + I_2 + l$. In any nuclear reaction this total angular momentum J is conserved, i.e. the total angular momentum quantum number J before the nuclear reaction is same as after the nuclear reaction. The law of conservation of total linear momentum, states that the total momentum before the nuclear reaction is same as the total momentum of the system after nuclear reaction and the total parity is also conserved.

The Q-value of any reaction is an important parameter that should be taken in to consideration while studying nuclear reaction.It is defined as the energy released or absorbed in the reaction.when a reaction take place energy mass equation for any reaction can be written as

$$X + x \longrightarrow Y + y \tag{2.2.1}$$

$$M_X C^2 + E_X + m_x C^2 + E_x \longrightarrow M_Y C^2 + E_Y + m_y C^2 + E_y \tag{2.2.2}$$

Generally target nucleus is stationry$E_x = 0$

$(M_X + m_x - M_Y - m_y)C^2 = E_Y + E_y - E_X = Q$

$$Q = (M_X + m_x - M_Y - m_y)C^2 \tag{2.2.3}$$

where

$M_X = is\ mass\ of\ the\ projectile$

$m_x = is\ mass\ of\ the\ target$

$M_Y = is\ mass\ of\ the\ residue$

$m_y = is\ mass\ of\ the\ emitted\ particle\ and\ C\ is\ speed\ of\ light\ in\ vacuum.$

Q may be positive or negative.If Q is positive, the reaction is said to be exoergic if Q is negative, it is endoergic.

2.3 Nuclear reaction Cross-section

Reaction cross-section is the most important quantity in nuclear reaction study. It is a measure of the the probability for particular reaction to occur. The larger the nuclear cross sections the more probable the reactions .This factor can be viewed as the target area effectively presented to the incident particles by each nucleus. such that if the incident particle passes through this area reaction will take place. The cross-section of a reaction is defined by :

$$\sigma = \frac{number\ of\ events\ of\ given\ type\ per\ unit\ time\ per\ nucleus}{number\ of\ incident\ particles\ per\ unit\ area\ per\ unit\ time} \tag{2.3.1}$$

Nuclear Cross-section or the probability of any interaction has dimention of Area that is so called Cross-section and measured in a unit of cm^2 or barn.

$1barn = 10^{-24}cm^2$

2.3.1 Some Semi-Classical Idea Of Reaction Cross-Section

If the bombarding particies has some impact parameter for the interaction, the value of impact parameter will decide whether the reaction will take place or not.

If P is linear momentum of the projectile and b is the impact parameter then Angular momentem is given as L=Pb. but from quantum mechanics Angular momentum is quantized and given as ℓh where ℓ=0,1,2... then by equating this two equation we can get b=$\ell\lambda$

where $\lambda = \frac{h}{P}$

This show that the quantization of Angular momentume gives the idea of quantization of impact parameter. which means the impact parameter for the beam will have discrete value and not continous value. All value of b are not possible b have the value 0,λ,2λ,3λ... All the particles in centeral zone of the beam have ℓ=0 and Impact parametre is less than λ. In the 1^{st} zone where impact parameter is in between λ and 2λ or ℓ=0
In ℓ^{th} zone all the particles moving will have impact parameter in between $\ell\lambda$ and (ℓ+1)λ. The Area of ℓ^{th} Zone Gives the Partial Cross-section.

$$\pi(\ell+1)^2\lambda^2 - \pi(\ell\lambda)^2 \tag{2.3.2}$$

Therefore from this reaction cross-section is

$$\sigma_r = \pi\lambda^2(2\ell+1) \tag{2.3.3}$$

2.3.2 Quantum mechanical plane wave analysis of reaction cross-section

Let us consider a collimated beam of neutrons falling on a target. The beam is moving in Z-direction this neutron beam can be considered as a plane wave

$$\psi_{inc} = e^{ikz} \tag{2.3.4}$$

The plane wave can be expanded interms of Bessels function and spherical harmonics of varies value of ℓ.

$$e^{ikz} = \sum_{\ell=0}^{\infty} i^{\ell}(2\ell+1)j_{\ell}(kr)P_{\ell}(cos\theta) \tag{2.3.5}$$

$$j_{\ell}(kr) = \frac{sin(kr - \frac{\ell\pi}{2})}{kr} \tag{2.3.6}$$

$$P_\ell(cos\theta) = \sqrt{\frac{4\pi}{2\ell+1}}\eta_{\ell,0},(\theta) \tag{2.3.7}$$

For $r \to \infty$ then the Bessel function $j_\ell(kr) = \frac{sin(kr-\frac{\ell\pi}{2})}{kr}$

$$e^{ikz} = \psi_{in} \tag{2.3.8}$$

$$\psi_{inc} = \frac{1}{kr}\sum_{\ell=0}^{\infty} i^\ell(2\ell+1)sin(kr-\frac{\ell\pi}{2})P_\ell(cos\theta) \tag{2.3.9}$$

$$\psi_{in} = \frac{1}{2ikr}\sum_{\ell=0}^{\infty} i^\ell(2\ell+1)[e^{i(kr-\frac{\ell\pi}{2})} - e^{-}i(kr-\frac{\ell\pi}{2}).P_\ell(cos\theta)] \tag{2.3.10}$$

$$\psi_{inc} = \frac{1}{2kr}\sum_{\ell=0}^{\infty}(2\ell+1)i^{\ell+1}[e^{-i(kr-\frac{\ell\pi}{2})} - e^{i(kr-\frac{\ell\pi}{2})}].P_\ell(cos\theta) \tag{2.3.11}$$

The 1^{st} term $e^{-i(kr-\frac{\ell\pi}{2})}$ is ingoing wave and the 2^{nd} term $e^{i(kr-\frac{\ell\pi}{2})}$ is outgoing wave. In the presence of a nucleus the amplitude of outgoing wave is modified.

$$\psi(r) = \frac{1}{2kr}\sum_{\ell=0}^{\infty}(2\ell+1)i^{\ell+1}[e^{-i(kr-\frac{\ell\pi}{2})} - \eta_\ell e^{i(kr-\frac{\ell\pi}{2})}]P_\ell(cos\theta) \tag{2.3.12}$$

$$\eta_\ell = \mid \eta_\ell \mid e^{i\delta\ell} \tag{2.3.13}$$

$e^{i\delta\ell}$ represents phase and $\mid \eta_\ell \mid$ is the amplitude.

If $\mid \eta_\ell \mid$ is changing, means amplitude is decreasing, reaction is taking place.

If δ_ℓ is changing then scattering is taking place.

If $\mid \eta_\ell \mid$ is not changing means no attenuation of amplitude and hence no reaction.

If the phase is changing (phase shift) then scattering is taking place.

The scattered wave can be written as

$$\psi_{sc} = \psi(r) - e^{ikz} \tag{2.3.14}$$

$$\psi_{sc} = \sum_{\ell=0}^{\infty} \frac{1}{2kr}(2\ell+1)i^{\ell+1}(1-\eta_\ell)(e^{i(kr-\frac{\ell\pi}{2})})P_\ell(cos\theta) \tag{2.3.15}$$

The scattered wave can be also written in terms of scattering amplitude as follows

$$\psi_{sc} = f(\theta)\frac{e^{ikr}}{r} \tag{2.3.16}$$

$f(\theta)$ is the scattering amplitude

Then to find the values of $f(\theta)$ simply compare the above two equations. Then

$$f(\theta) = \sum_{\ell=0}^{\infty} \frac{i^{\ell+1}}{2k}(2\ell+1)e^{\frac{-i\ell\pi}{2}}(1-\eta_\ell)P_\ell(cos\theta) \tag{2.3.17}$$

$$i^\ell e^{\frac{-i\ell\pi}{2}} = 1 \tag{2.3.18}$$

For any value of ℓ

$$f(\theta) = \frac{1}{2ik}\sum_{\ell=0}^{\infty}(\eta_\ell - 1)P_\ell(cos\theta)(2\ell+1) \tag{2.3.19}$$

To get the scattering cross-section, we consider a sphere of radius r_0 enclosing the scatterer.

The values of r_0 is very much larger than the nuclear force range.

The number of scattered particle through the solid angle $d\Omega$ is equal to the number of particles scattered through $r_0^2 d\Omega$.

N_{sc} can be calculated using the expression of the probability of current density.

$$N_{sc} = \frac{\hbar}{2mi}\int (\frac{d\psi_{sc}}{dr}.\psi_{sc}^* - \frac{d\psi_{sc}^*}{dr}.\psi_{sc})_{r=r_0}^{r_0^2 sin\theta d\theta d\phi} \tag{2.3.20}$$

$$\frac{\hbar k}{m} = \hbar\frac{\sqrt{2mE}}{\hbar m} = \frac{\sqrt{2mE}}{m} \tag{2.3.21}$$

$$k = \frac{\sqrt{2mE}}{\hbar} \tag{2.3.22}$$

$$v = \frac{\sqrt{2E}}{\sqrt{m}} = \frac{\sqrt{2mE}}{m} \tag{2.3.23}$$

$$N_{SC} = \frac{\hbar k}{m} \int \mid f(\theta) \mid^2 sin\theta d\theta d\phi \tag{2.3.24}$$

Where m is the mass number of incident particle

$$v \int \mid f(\theta) \mid^2 d\Omega \tag{2.3.25}$$

$$N_{sc} = \frac{v\pi}{k^2} \sum_{\ell=0}^{\infty} (2\ell + 1) \mid 1 - \eta_\ell \mid^2 \tag{2.3.26}$$

Due to orthogonality of spherical harmonics and legendere polynomial

$$P_\ell(cos\theta) = \sqrt{\frac{4\pi}{2\ell + 1}} \eta_{\ell m} \tag{2.3.27}$$

$$\sigma_{sec} = \frac{N_{sc}}{Incident\ flux} \tag{2.3.28}$$

Incident flux for a plane wave e^{ikz} moving with velocity v

$$\int \psi\psi^* d\tau = 1 \tag{2.3.29}$$

Particle density in a plane wave is the flux of plane wave number of particle per second per unit area=v then

$$\sigma_{sc} = \frac{N_{sc}}{Incident\ flux} \tag{2.3.30}$$

$$\sigma_{sc} = \frac{N_{sc}}{v} = \frac{\pi}{k^2} \sum_{\ell=0}^{\infty} (2\ell + 1) \mid 1 - \eta_\ell \mid^2 \tag{2.3.31}$$

From the relation

$$P = \frac{\hbar}{\lambda} = \hbar k \tag{2.3.32}$$

$$\sigma_{sc} = \pi\lambda^2 \sum_{\ell=0}^{\infty}(2\ell+1) \mid 1-\eta_\ell \mid^2 \tag{2.3.33}$$

$$\sigma_{sc,\ell} = \pi\lambda^2(2\ell+1) \mid 1-\eta_\ell \mid^2 \tag{2.3.34}$$

Then let calculate the reaction cross section using the probablity current density expression.

now first let calculate number of particles going in

$$N_r = -\iint \frac{\hbar}{2mi}(\frac{d\psi_r}{dr}.\psi_r^* - \frac{d\psi_r^*}{dr}.\psi_r)r_0^2 sin\theta d\theta d\phi \tag{2.3.35}$$

In place of ψ_{sc} we have ψ_r

$$\frac{\hbar\pi}{mk}\sum_{\ell}(2\ell+1)(1- \mid \eta_\ell \mid^2) \tag{2.3.36}$$

$$\sigma_r = \frac{N_r}{incident flux} = \frac{N_r}{v} \tag{2.3.37}$$

$$\sigma_r = \frac{N_r}{v} = \frac{\pi}{k^2}\sum_{\ell=0}^{\infty}(2\ell+1)(1- \mid \eta_\ell \mid^2) \tag{2.3.38}$$

$$\sigma_r = \pi\lambda^2 \sum_{\ell=0}^{\infty}(2\ell+1)(1- \mid \eta_\ell \mid^2) \tag{2.3.39}$$

Then the total cross section $\sigma_{t,\ell}$ is given as

$$\sigma_{t,\ell} = \sigma_{sc,\ell} + \sigma_{r,\ell} \tag{2.3.40}$$

$$\sigma_{t,\ell} = \pi\lambda^2(2\ell+1)[1- \mid \eta_\ell \mid^2 + \mid 1-\eta_\ell \mid^2] \tag{2.3.41}$$

$$\sigma_{t,\ell} = \pi\lambda^2(2\ell+1)[1-\eta_\ell\eta_\ell^* + (1-\eta_\ell)(1-\eta_\ell^*)] \tag{2.3.42}$$

$$\sigma_{t,\ell} = \pi\lambda^2(2\ell+1)[2-\eta_\ell-\eta_\ell^*] \tag{2.3.43}$$

$$\sigma_{t,\ell} = \pi\lambda^2(2\ell+1)[2-(Re\eta_\ell+Img\eta_\ell)-(Re\eta_\ell-Img\eta_\ell)] \tag{2.3.44}$$

$$\sigma_{t,\ell} = \pi\lambda^2(2\ell+1)[2-2Re\eta_\ell] \tag{2.3.45}$$

$$\sigma_{t,\ell} = 2\pi\lambda^2(2\ell+1)[1-Re\eta_\ell] \tag{2.3.46}$$

Note $1-Re\eta_\ell = 2sin^2\delta\ell$

Total cross section is given by only $Re\eta_\ell$

$$\eta_\ell = \mid \eta_\ell \mid e^{2i\delta\ell} \tag{2.3.47}$$

If $\mid \eta_\ell \mid = 1$

$\eta_\ell = e^{i2\delta\ell} = cos2\delta\ell + isin2\delta\ell$

then the real part of $\eta_\ell = Re\eta_\ell = cos\delta\ell$

$1-Re\eta_\ell = 2sin^2\delta\ell$

$$\sigma_{t,\ell} = 2\pi\lambda^2(2\ell+1)2sin^2\delta\ell = 4\pi\lambda^2(2\ell+1)sin^2\delta\ell \tag{2.3.48}$$

$$\sigma_{r,\ell} = \pi\lambda^2(2\ell+1)(1-\mid \eta_\ell \mid^2) \tag{2.3.49}$$

$$\sigma_{sc,\ell} = \pi\lambda^2(2\ell+1) \mid 1-\eta_\ell \mid^2 \tag{2.3.50}$$

$\mid \eta_\ell \mid = 1$ for this case $\sigma_{r,\ell} = 0$ but $\sigma_{sc,\ell}$ may be finite as η_ℓ is complex.

For $\eta_\ell = 1$ then $\sigma_{sc,\ell} = 0$, $\sigma_{r,\ell} = 0$

For $\eta_\ell = -1, \sigma_{r,\ell} = 0$, $\sigma_{sc,\ell_{max}} = 4\pi\lambda^2(2\ell+1)$

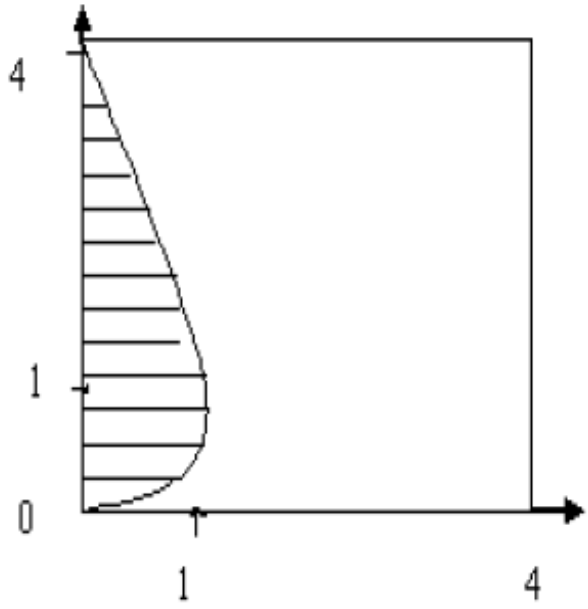

Figure 2.1: Comparision of reaction cross-section and scattering cross-section

For $\eta_\ell = 0, \sigma_{r,\ell_{max}} = \sigma_{sc,\ell} = \pi\lambda^2(2\ell+1)$

$\mid \eta_\ell \mid = 1$ then $\sigma_{r,\ell} = 0$, $\sigma_{sc,\ell} = finite$

The vertical axise represents $\frac{\sigma_{sc,\ell}}{\pi\lambda^2(2\ell+1)^2}$ and

The horizontal axise represents $\frac{\sigma_{r,\ell}}{\pi\lambda^2(2\ell+1)^2}$

When reaction cross-section is zero, scattering is also zero and when reaction cross-section is maximum at $\mid \eta_\ell \mid = 0$ scattering cross-section is equal to reaction cross-section.

When scattering is maximum, reaction is zero.

No reaction possible with out scattering or scattering is always associated with reaction.

Reaction is zero when scattering is maximum.

Scattering is possible with out reaction but no reaction is possible with out scattering.

$$\sigma_{r,\ell} = \pi\lambda^2(2\ell+1)(1- \mid \eta_\ell \mid^2) \tag{2.3.51}$$

At the absolute value of η_ℓ=0

$$= \sigma_{r_{max}} + \sigma_{sc} = 2\pi\lambda^2 \sum_{\ell}^{\ell_m}(2\ell+1) \tag{2.3.52}$$

$$\sigma_t = 2\pi\lambda^2(\ell_m + 1)^2 \tag{2.3.53}$$

Where $\ell_m = \frac{R}{\lambda}$

$$\sigma_t = 2\pi\lambda^2(\frac{R}{\lambda} + 1)^2 = 2\pi\lambda^2\frac{(R+\lambda)^2}{\lambda^2} \tag{2.3.54}$$

$$\sigma_t = 2\pi(R + \lambda)^2 \tag{2.3.55}$$

For high energy $R >> \lambda$

$$\sigma_t = 2\pi R^2 \tag{2.3.56}$$

Total cross-section is twice of the geometrical cross-section of the nucleus.

2.4 REACTION MECHANISMS

In a projectile target nucleus interaction either of two things may happen. The projectile may simply be deflected by the target nucleus potential and change its direction without any change in the center of mass energy. This is shape elastic scattering. On the other hand, the projectile may interact with target particle, lose energy to it and thus be removed from the entrance channel to be absorbed by the target nucleus. After the absorption nuclear reaction may occur by any of three processes, viz, direct reaction mechanism, compound nuclear emission or by pre-equilibrium emissions. If the projectile enters the nucleus and interacts with one nucleon (or a cluster) and both of them are ejected after a single interaction this is called direct reaction. If the projectile interacts with a limited number say 2 to 5 nucleons, before the striking projectile and or the ejectiles come out, this is a case of pre-compound reaction mechanism. On the other hand, the incident projectile may interact with a large number say thousands or more of the nucleons, inside the nucleus in some sequence and the energy of the incident particle is shared by a very large numbers of nucleons, so that only after a lot of interactions including many reflections from the surface, some nucleons (or clusters) find enough energy and

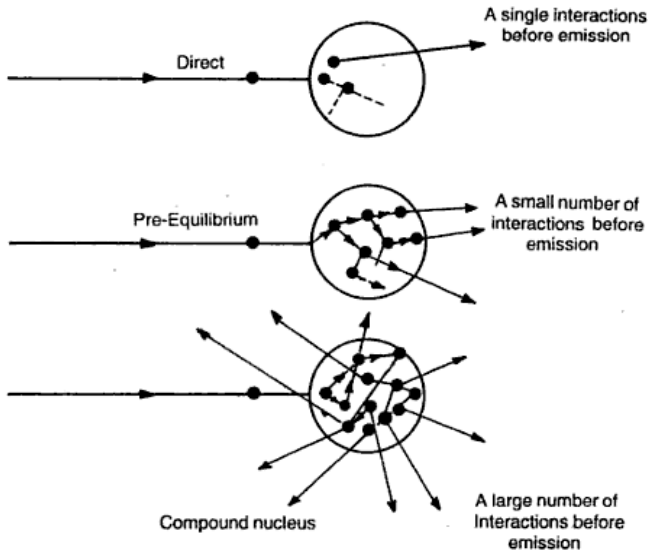

Figure 2.2: Three models of reaction mechanism. In the direct mode, there is only one interaction; in pre-compound 2-4 or 5 and in compound several thousand interaction before emission.

get emitted. This scenario corresponds to the compound nucleus formation [5].

In general,these reactions can be classified according to the time scale on which they occur, and the degree to which the kinetic energy of the incident particle is converted into internal excitation of the final products. The interaction of a projectile with a nucleus may exhibit several effects.

The simplest form is the formation of the compound nucleus which can be described by statistical mechanics as being in a state of statistical equilibrium. The energy distribution of the components of the system is Maxwellian. A component of this system may get a large amount of energy as a result of the statistical fluctuation. This amount of energy may enough to cause the decay of the compound nucleus. Being a statistical process, the evaporation of particles favors the escape of nucleons having the minimum possible energy. In case of charged particles, this minimum energy is the Coulomb barrier of the compound nucleus. When the compound nucleus has reached statistical equilibrium, it is

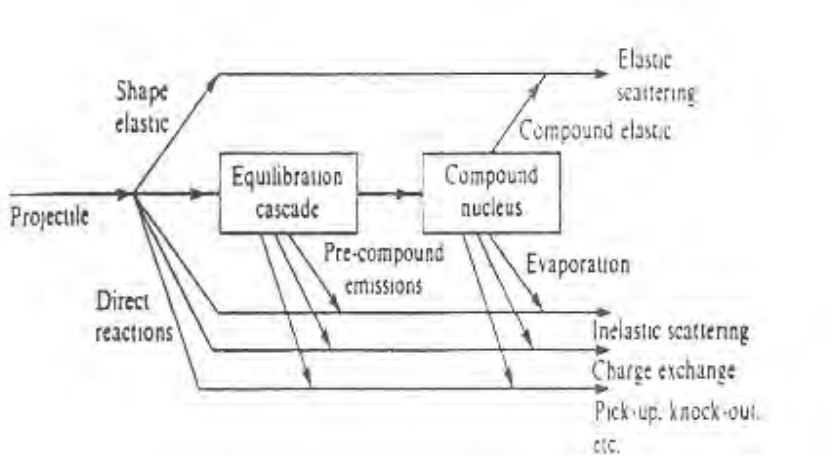

Figure 2.3: An overview of all possible nuclear reaction mechanisms

said to have been thermalized.

If the nuclear reactions proceed directly from the entrance channel to the exit channel without the formation of an intermediate state, they are said to be direct reactions. If the internal states of the two colliding systems do not change, we have elastic scattering and if one or both systems are excited in the exit channel, it is inelastic scattering. An overview of all possible nuclear reaction mechanisms is given as above in Fig(2.3)

2.4.1 Direct reaction mechanism

Nuclear reaction may take place only with certain parts of the target nucleus being the rest undisturbed. A direct reaction takes place when the projectile interacts primarily with the nucleons in the surface of the target nucleus. The interaction is with one or two nucleons. Energy and momentum transfer is very small and the transfer is to only few nucleons and emission of the particle most probably is in direction of motion of the projectile. The reaction which take place with out the formation of compound nucleus are called direct reaction.

In any case the projectile interacts with only a small portion of the nucleus with the

consequence that the ejectile takes up a substantial part of the projectile momentum. The projectile energy is then high and the residual nucleus is left at comparatively low excitation where the nuclear states are discrete. The ejectile spectrum is, therefore, also discrete. One property which distinguishes this type of reaction,direct reaction, from the compound nucleus reaction is that it proceeds much more rapidly, in time of the order of the nuclear transit time about 10^{-21}s.

Unlike compound nucleus theory,experiments show that the differential cross section of certain type of reaction is strongly peaked in the forward direction. This may be accounted for if it is assumed that some of the incident particles interact with nucleons in the equatorial rim of the target nucleus. In doing so they loose some energy and are deflected through a small angle but not captured into the compound nucleus. When the incident particles are positively charged,some of them which also interact with the interior of the nucleus will be reflected back by the Coulomb barrier until they are captured into the compound nucleus [16].However,this compound nucleus will decay predominantly through the emission of neutron, so that the compound process is dominant in the (p,n) reaction. The direct reaction process involves a single-step interaction between the projectile and a target particle (single nucleon or cluster). The wave functions involved are comparatively simple and standard one body wave equations can be used to analyze the ejectile spectrum and angular distribution. Also, since the projectile energy and momentum govern the kinematics of the interaction leading to direct emissions, the ejectile angular distribution is strongly forward peaked [17]. If we take the target nucleus to be moderately absorptive so that direct reaction takes place throughout the nuclear surface,the interference in the surface of the nucleus may be studied with a simple geometrical representation.

Let K_i be the incident wave vector and K_f is the wave vector of emitted particle at an angle θ from the initial direction. Then the angular momentum transfer vector is $L = \hbar q \times r = \hbar(K_i - K_f) \times r$ where r is the position vector at the point of interaction of the incident and the target particle(nucleons) and q is the linear momentum transfer.

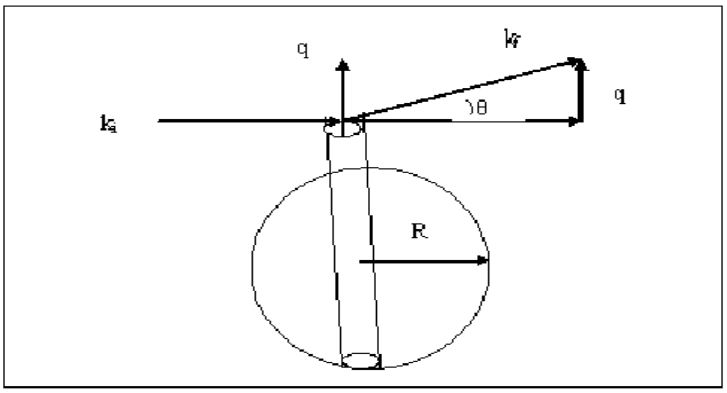

Figure 2.4: Interference in direct interaction in the surface of the nucleus Ref[18]

From the vector diagram as shown in the figure(2.4), we can write

$$q^2 = K_i^2 + K_f^2 - 2K_iK_fcos\theta \tag{2.4.1}$$

for stripping reaction like (d,p) the q may be the linear momentum transferred to target nucleus by absorbed neutron.we can write $K_i = K_d, K_f = K_p$ and $q = K_n$

We can write Eqn.(2.4.1) for (d,p) reaction

$$K_n^2 = K_d^2 + K_p^2 - 2K_dK_pcos\theta \tag{2.4.2}$$

The angular momentum transfer by absorbing neutrons is given by:

$$L_n = \hbar(K_n \times r) \tag{2.4.3}$$

L_n must be an integral value(integer multiple of $\hbar$) i.e.$L_n = l_n\hbar$ where l_n=0,1,2,.....

As r is perpendicular to the linear momentum vector K_n,we can write:

$$K_nr = K_nRsin\beta = l_n$$

or

$$\frac{l_n}{K_n} = Rsin\beta$$

for $\beta = 90$

$$\frac{l_n}{K_n} \leq R \tag{2.4.4}$$

0r

$$\frac{K_n^2}{l_n^2} \geq \frac{1}{R^2} \tag{2.4.5}$$

$$\frac{K_d^2 + K_p^2 - 2K_dK_pcos\theta}{l_n^2} \geq \frac{1}{R^2} \tag{2.4.6}$$

or

$$cos\theta \leq \frac{K_d^2 + K_p^2}{2K_dK_p} - \frac{l_n^2}{2K_dK_pR^2} \tag{2.4.7}$$

For given values of the energy of the deutron and proton which determines the value of K_d and K_p for a given nucleus(given R). Eqn.(2.4.7) can calculate the emission angle of proton and sets an upper limit to the value of $cos\theta$ or lower limit to θ,the angle at which proton is emitted. In Eqn.(2.4.7) if $K_d^2 + K_p^2 \geq 2K_dK_p$ the first term more than 1.suppose the second term is zero due to $l_n = 0$ and if the first term is 1,$\theta = 0$. The angle of emission of proton is $\theta = 0$. But if $l_n = 1, 2, 3, ..$, second term give some negative contribution which will make $cos\theta$<1 and angle θ increases from 0.

The angle θ is increasing with l_n value,i.e. angular momentum transfer to the nucleus.The quantum mechanical theory of direct reaction was given by N.Austerts and S.T.Butlar. They have shown that the differential cross-section is proportional to the modules square of spherical Besseles function.i.e.

$$\sigma \propto |j(KT)|^2 \tag{2.4.8}$$

where $j(KT)$ is spherical Bessel function.Some direct interaction angular distributions are shown in Fig.(2.5) taken from Ref.[19].

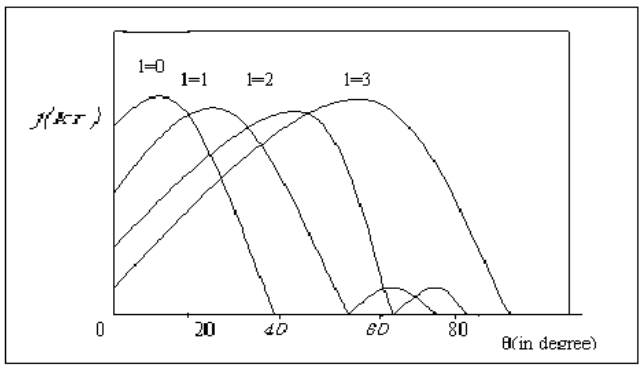

Figure 2.5: Direct interaction angular distributions

2.4.2 The compound Nucleus reaction

At the other extreme we have the compound nuclear reactions these reactions are important at comparatively low incident energies. In this case there is no emission after a single interaction. Instead both the projectile and the excited nucleon (or cluster) remain inside the nucleus and undergo further interactions inside the nuclear matter. Through successive interactions the energy and momentum brought in by the projectile are diffused through the nucleus and eventually transferred to the composite nucleus as a whole. During the process of energy-momentum sharing more and more degrees of freedom are excited after each interaction with the consequence that the nuclear state becomes more and more complex. After certain relaxation time a condition of statistical equilibrium is reached when the average number of excited degrees of freedom becomes constant .At statistical equilibrium, different nuclear configurations arise and decay in to other configurations. A certain fraction of the equilibrium configuration consists of configurations in which sufficient energy is concentrated on a single nucleon (or cluster) so that it may be emitted from the nucleus.

A compound nucleus is formed when the composite nucleus attains statistical equilibrium and emissions taking place through statistical fluctuations from the equilibrium configuration are called compound nuclear emissions. A nuclear reaction of this type is described

as: $x + X \rightarrow C^* \rightarrow Y + y$. On nuclear time scale this takes a considerable time, which is about $(10^{-13} - 10^{-16}\text{s})$. Once equilibrium is reached the compound nucleus retains no memory of its mode of formation and the decay modes of the compound nucleus are the very general ones. The ejectiles come out with low energies the residual nucleus is left with comparatively high excitation where the density of nuclear levels is large. So the ejectile spectrum is continuous.

According to the Bohr assumption, We can Write the probability of formation of compound nucleus $\sigma_c(a)$ and the probability of a decay of compound nucleus Y and emitted particles b of a nuclear reactions X (a,b)Y in the form

$$\sigma(a, b) = \sigma_c(a) G_c(b) \tag{2.4.9}$$

Where, $\sigma_c(a)$ is the cross sections for the formation of a compound system by particle a incident up on the target nucleus X. Gc (b) is the probability that the compound system C, once formed , decay by emission of a particles b, leaving a residual nucleus Y. Gc (b) is a pure number; the compound system C must decay eventually in some way; $G_C(b)$ is the probability of this special way of decay. It can also be referred to as the branching ratio of the reaction in to the emission of b.

Evidently

$$\sum G_c(b) = 1 \tag{2.4.10}$$

if the sum is extended over all particles b which C can emit.

It is useful to specify the reaction X (a,b) Y in greater detail, by considering the cross section $\sigma(\alpha, \beta)$ corresponding to a specific entrance channel α and specific exit channel β. In other words, we specify the quantum states of all reactions partners before and after the reaction [20].

We therefore write

$$\sigma(\alpha, \beta) = \sigma_c(\alpha) G_c(\beta) \tag{2.4.11}$$

Where $\sigma_c(\alpha)$ is the cross section for the formation of C channel α, and $G_c(\beta)$ is the probability that C decays through channel β.

According to the Bohr assumption, the disintegration of the compound system in to the different channels β, γ, etc.,depends only on the energy E_c, the angular momentum J_c , and the parity of the compound system.

In order to simplify our present consideration, the dependence of the properties of the compound system on the angular momentum J and the parity Π will be ignored in this section. We now introduce a few magnitudes which describe the disintegration of the com pound system C. We begin with the mean life time $\tau(E_c)$ of C before disintegration and define the magnitude.

$$\Gamma(E_c) = \frac{\hbar}{\tau(E_c)} \tag{2.4.12}$$

Which is $\hbar$ times the rate of disintegration per unit time.

Γ is an energy and, later on, will play the role of a level width. We therefore call it the total width of the state of C with an excitation energy E_c. C can decay in to several channels, and its total decay rate Γ can therefore be subdivided in to decay rates referring to specific channels.

$$\Gamma(E_c) = \sum \Gamma_\beta(E_c) \tag{2.4.13}$$

Where the sum is extended over all channels in to which C can decay, i.e., over all open channels. The specific decay rate $\Gamma(E_c)$ is also a function of E_c and is called the partial width for the decay in to channel .

The magnitude Γ_β can also be defined as follow:

If an assembly of N equal samples of the compound system C is arranged in such away that, on the average, N system constant in time (i.e. as many compound systems decay as are produced), then the number of decays in to channel β per unit time is given by

$$\frac{N\Gamma_\beta}{\hbar} \tag{2.4.14}$$

We can now express the branching probability in terms of the decay rates by the relation

$$G_c(\beta) = \frac{\Gamma_\beta}{\Gamma} \tag{2.4.15}$$

The reaction time for compound nuclear emissions is of the order of the relaxation time. A perturbation of nuclear matter has a typical propagation velocity of the average nucleon velocity inside the nuclear matter.

If v and l be the average nucleon velocity and the mean free path respectively, inside the nucleus, then the average number of interactions per unit time is v/l. If N interactions are necessary to reach the statistical equilibrium then Nl/v is the time taken to form the compound nucleus. The relaxation time may then be expected to be one or two orders of magnitude longer than the time taken for direct reactions. The direct and compound nuclear reactions taken together can account for the greater part of the nuclear reaction cross-sections. However, these are not the only mechanisms by which particle emission can occur in nuclear reactions[21].

2.4.3 Pre-equilibrium reaction

Pre-equilibrium reaction is neither direct nor compound nucleus reaction. In this type of reactions particles are emitted after the first stage of a nuclear interaction(direct reaction)but long before the attainment of statistical equlilibrium(compound nucleus formation). Their time scale is intermediate between the very fast direct reactions and the relatively slow compound nucleus formation.

Many recent heavy-ion experiments have provided evidence for non-equilibrium particle emission. In order to interpret the physical message of the experimental observations it is necessary to have an appropriate reaction model. Suitable models for heavy-ion pre-compound decay phenomena may provide the necessary bridge in understanding the transition between low energy compound nucleus reaction and the fragmentation reactions of higher incident energies.

Among the several semi-classical models which have been proposed in reproducing a large

body of experimental data are the hybrid and Geometery Dependent Hybrid models. They have been reasonably successful in reproducing a broad range of expermental data.This was accomplished with several choices of parameter options.

Recently quantum mechanical theories of pre-equilibrium emission have been proposed. These quantum mechanical models[16] provide,in principle,way of calculating the cross-sections of pre-equilibrum processes with out the uncertainties of the semi-classical approximations. These models are in the early stage of application,at the present. Even for light heavy-ion particle alpha,the quantum mechanical treatement of the initial particle-target interaction become very complicated.Now we will see some of these models in the following sub-section

- **Exciton model**

The exciton model, first introduced by Griffin[22] and later modified by many workers, the composite nucleus states are characterized by the number of excited particles and holes (the exciton) at every stage of the nucleon-nucleon cascade. In this model the equilibration between target and projectile is achieved by the succession of nucleon-nucleon interactions.The initial configuration is fixed by the nature of the projectile. For example in the case of a nucleon-induced reaction, it is a two-particle and one-hole configuration due to the interaction of the incident nucleon with a nucleon of the target which is excited from a state below to a state above Fermi energy. Additional nucleon-nucleon interactions give rise to a sequence of states characterized by increasing exciton numbers, eventually leads to a fully equilibrated residuals nucleus. A typical graph illustrating the simple exciton model is illustrated in fig 2.6. Initially the target nucleus is in the ground state. All the levels below the fermi energy are filled and all the levels above are vacant.

The projectile nucleons enter the target nucleons with a given energy and form 1 particle - 0 hole (1p0h) states. In this case n=1 as can be seen in fig 2.6(a) at this stage, the projectile has entered the nuclear force field but has not been absorbed by the target. It

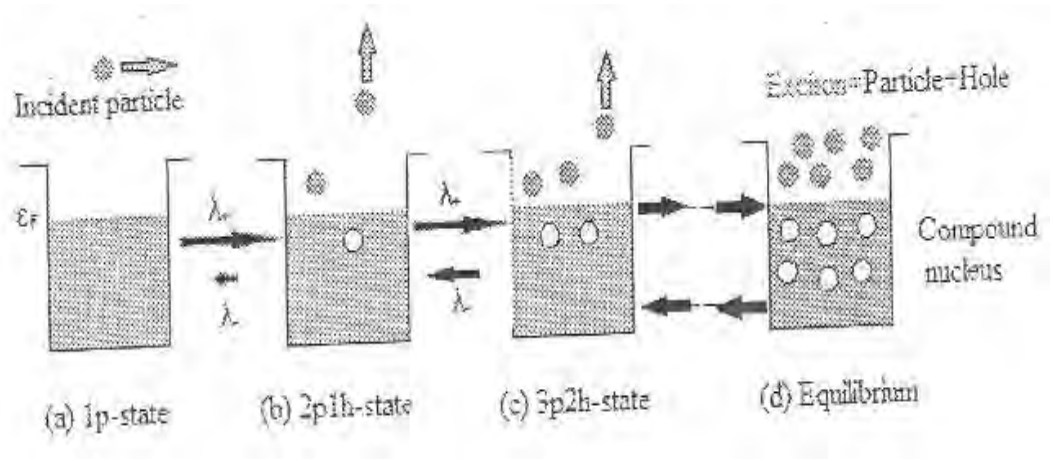

Figure 2.6: A typical diagram illustrating a nucleon-induced Exciton model.

is still in the entrance channel and can leave the nuclear force field without interacting with any individual target nucleon. Since all levels below the fermi energy are filled, the first interaction (absorption by the target) between the projectile and target nucleon will rise the later above the fermi energy and leave a hole below. Thus 2p1h state is formed i.e., a state with exciton number n=3 state either of the excited particles may be emitted if it has sufficient energy to escape. If however, particle emission does not take place, and then there will be a further two body interaction either between one of the excited particle and a nucleon below fermi sea or between the two excited particles themselves. The first process leads to the formation of n=5 (3p2h) state while the second would produced a new state n=3 (2p1h) state having different energy configuration of the hole and particles, or back to the original n=1 exciton state. Restrictions to two-body interactions lead to the following selections rules concerning the possible variation of the number of particles p, holes h, and exciton n=p+h, in the course of the cascade of interactions: $\Delta p = 0, \pm 1, \Delta h = 0, \pm 1, \Delta n = 0, \pm 2$.

The states which are excited in the course of this interaction cascade are very unstable. In exciton model intermediate states play significant role in dealing PE processes. Single particles densities are often used to calculate the exciton level densities, assuming the nucleus to be distinguishable fermi gas with equidistance level. The transition rates are

proportional to level density of the final accessible states (Fermi Goldens rule). Ericson's level density result, at a given exciton number n, with excitation energy E_{ex} is:

$$\rho_n(E_{ex}) = \frac{g(gE_{ex})^{p+h-1}}{p!h!(p+h-1)!} \tag{2.4.16}$$

In this equation g is the one-particle state density, E_{ex} is the excitation energy, and p and h are the numbers of excited particles and holes. Wiliam gave expression for the particle-hole density by considering the effect of the pauli Exclusion principle in the uniform spacing model as

$$\rho_n(E_{ex}) = \frac{g(gE_{ex} - A(p,h))^{p+h-1}}{p!h!(p+h-1)!} \tag{2.4.17}$$

Here $A(p,h) = \frac{1}{2}(p^2 + h^2 + p - h) - \frac{1}{2}h$

The probability of decay from an n exciton state $P_n(E_{ex})$ is defined as the ratio of the emission rate from n to the rates of all transitions (including emission) from n. If $\lambda_c^n(\varepsilon)$ be the emission rate with energy ε (in the interval $d\varepsilon$) from the n exciton state and $\lambda_{\pm,0}^n$ the rates for the transitions corresponding to the change of the exciton number $\Delta n = \pm 2, 0$

$$P_n(\varepsilon) = \frac{\lambda_c^n(\varepsilon)}{\lambda_+^n + \lambda_-^n + \lambda_0^n + \int d\varepsilon \lambda_c^n(\varepsilon)} \tag{2.4.18}$$

The exciton model assumes that

i) at each stage of the cascade all the states with the same configuration and the same total energy are equiprobable, and

ii) at each stage of the cascade all the processes which may occur are also equiprobable . The first assumption implied that partitioning of energy occurs with equal apriori probability. Hence emission rates are summed over all ε in the denominator to obtain $P_n(\varepsilon)$. The emission rate as obtained from the principle of detailed balance is given by

$$\lambda_c^n(\varepsilon) = \frac{(2s+1)}{\hbar}[\frac{\rho_{n'}(u)}{\rho_n(E_{ex})}]m\varepsilon\sigma_{inv}(\varepsilon) \tag{2.4.19}$$

Here s and m are the intrinsic spin and reduced mass of the ejectile,n' is the exciton number after emission of ejectile with v nucleons: $n' = n - v$, u is the residual excitation

energy given by $u = E_{ex} - B - \varepsilon$, with B the ejectile separation energy, σ_{inv} is the inverse cross-section. Using Fermi's-golden rule the transition rates are defined as

$$\lambda_+^n = \frac{2\pi}{\hbar}|M_+|^2\rho_{n+2}, \Delta n = +2 \tag{2.4.20}$$

$$\lambda_-^n = \frac{2\pi}{\hbar}|M_-|^2\rho_{n-2}, \Delta n = -2 \tag{2.4.21}$$

$$\lambda_0^n = \frac{2\pi}{\hbar}|M_0|^2\rho_n, \Delta n = 0 \tag{2.4.22}$$

Here $|M_{0,\pm 2}|$ are the matrix element of the corresponding transitions ρ_{n+2} , ρ_{n-2} and ρ_n are the density of states available in the n+2, n-2 and n exciton states after $\Delta n = 2, -2$ and 0 transitions. The estimation of the transition matrix element proves to be one of the most crucial points in the model. A common estimation is to assume $M_+ = M_- = M0 = M$. Using the assumption and the consequent restriction imposed on the density of final states, the transition states were given by Williams as

$$\lambda_+ = \frac{2\pi}{\hbar}|M|^2\frac{g^3E^2}{2(n+1)}, \Delta n = +2 \tag{2.4.23}$$

$$\lambda_- = \frac{2\pi}{\hbar}|M|^2 gph(n-2), \Delta n = -2 \tag{2.4.24}$$

$$\lambda_0 = \frac{2\pi}{\hbar}|M|^2 g^2 E\frac{3n-2}{4}, \Delta n = 0 \tag{2.4.25}$$

Where E is the excitation energy of the system.The matrix element is evaluated empirically.The most common form of $|M|^2$ empirical results for nucleon-nucleon scattering is given by Kalbach .

$$|M|^2 = \frac{k\sqrt{\frac{e}{7Mev}}\sqrt{\frac{e}{2Mev}}}{eA^3} \tag{2.4.26}$$

for $e < 2Mev$

$$|M|^2 = \frac{k\sqrt{\frac{e}{7Mev}}}{eA^3} \tag{2.4.27}$$

for $2Mev \leq e \leq 7Mev$

$$|M|^2 = \frac{k\sqrt{\frac{15Mev}{e}}}{eA^3} \tag{2.4.28}$$

for $e \geq 15Mev$

where $e = \frac{E}{n}$ and $k = 135Mev^3$

Compound nuclear equilibration is attained when the rate of creation of p-h pairs approximately equals the annihilation rates of such pair, so that the exciton number $n = \bar{n}$ remains unchanged. Assuming that λ_{n+2}=λ_{n-2}=λ_0 at equilibrium i.e.,$n = \bar{n}$ it follows

$$\bar{n} \cong \sqrt{2gE} \tag{2.4.29}$$

At low excitation energy, it is reasonable to assume energy independent matrix element. While at higher excitation energies, energy dependent matrix elements are used. The analysis of a large body of data indicates that a mass and energy dependence of the average square matrix for nucleon-nucleon interaction given by kalbach's estimate , according to which $|M|^2$ has the following mass number (A) and energy (E_{ex}) dependent

$$|M|^2 = KA^{-3}E_{ex}^{-1} \tag{2.4.30}$$

Where K is an adjustable parameter ranging from 95-700 Mev^3

• The Hybrid model

The Hybrid model was proposed by Blann [11].Predictions of pre-equilibrium decay in heavy ion reaction where made a decay ago using the hybrid model.The pre-equilibrium decay probability is given by

$$P_v(\varepsilon)d\varepsilon = \sum_{n=n_o,\Delta n=+2}^{\bar{n}} [\frac{nX_nN_n(\varepsilon,u)}{N_n(E)}]gd\varepsilon * [\frac{\lambda_c^n(\varepsilon)}{\lambda_c(\varepsilon)+\lambda_+(\varepsilon)}]D_n \tag{2.4.31}$$

Here $P_v(\varepsilon)d\varepsilon$ is the number of particles of the type v emitted in to the unbounded continuum with channel energy between ε and $\varepsilon + d\varepsilon$.

The quantity in the first bracket of Eq (2.4.31) represents the number of particles to be found (per Mev) at a given energy ε (with respect to continuum) for all scattering processes leading to an "n" exciton configuration. The nucleon-nucleon scattering energy

partition function $N_n(E)$ is identical to the exciton state density $\rho_n(E_{ex})$ and $N_n(E)$ represent number of combination with which n exciton may share E_{ex}.

The second set of bracket in Eq (2.4.31) represents the fraction of the v type particles at energy ε which should undergo emission in to the continuum, rather than making an inter-nuclear transition. The D_n represents the average fraction of the initial population surviving to the exciton number being treated. The H model calculates the nucleon-nucleon interaction rate $\lambda_+(\varepsilon)$ from the nucleon-nucleon scattering cross-section. Blann gave the empirical expression for the two-body interaction rates[23] as follows:

$$\lambda_+^n = [1.4 * 10^{21}(\varepsilon + B_{sp}) - 6 * 10^{18}(\varepsilon + B_{sp})^2]k^{-1} \tag{2.4.32}$$

Where ε is the particle energy outside the nucleus i.e., ejectile energy and B_{sp} its separation energy k is an adjustable constant and λ_+^nrepresents the rate at which a nucleon at a given energy $\varepsilon + B_{sp}$ above the Fermi energy undergoes two-body interactions.

- **Geometry Dependent Hybrid model**

Geometry dependent hybrid (GDH) model have been reasonably successful reproducing a broad range of data. This was accomplished with several choices of parameter options. The geometry dependent hybrid model is a variant of the HM in which the nuclear geometry effects are considered. GDH model takes in to account the reduced matter density and hence also the shallow potential. In this way the diffused surface properties sampled by higher impact parameter were incorporated in to the pre-compound decay formalism in the geometry dependent hybrid model.

The nucleon density distribution in the nuclear skin can affect the pre-equilibrium decay in two ways. First the mean free path in the intranuclear transitions is greater in the diffused edges and secondly the Fermi energy will be lower in that region so that the hole depth is limited. Considering these effects the Hybrid model for the cross sections was

reformulated as a sum of contributions over impact parameter[23].

$$\sigma_v(\varepsilon)d\varepsilon = \frac{\pi}{k^2}\sum_{l=0}^{\infty}(2l+1)T_l P_v(\varepsilon)d\varepsilon \tag{2.4.33}$$

Where $P_v(\varepsilon)$ is the pre-equilibrium decay probability calculated as a function of nuclear density and T_l is the transmission coefficient. The differential emission spectrum is given in the GDH model as

$$\frac{d\sigma_v(\varepsilon)}{d\varepsilon} = \pi\lambda^2\sum_{l=0}^{\infty}(2l+1)T_l P_v(l,\varepsilon) \tag{2.4.34}$$

Where $P_v(l,\varepsilon)d\varepsilon$ is as for $P_v(\varepsilon)d\varepsilon$, but evaluated for the l^{th} partial wave. T_l is the transmission coefficient for the l^{th} partial wave, and λ is the reduced de-Brolie wave length.For the calculation of the nuclear density the Fermi distribution may be applied as used by M. Blann [23].

$$d(R) = \frac{\bar{d}}{[e^{\frac{R-c}{z}}+1]} \tag{2.4.35}$$

Where $d(R)$ is the nuclear matter density at radius R, $\bar{d}$ is the central nuclear density,c is the charge radius with

$$c = 1.07A^{\frac{1}{3}}fm$$

and $z = .55fm$. The transition rates in the Hybrid model in each region is multiplied by $\frac{\bar{d}}{<d(r)>}$ to include all impact parameters. Where $< d(R) >$ represent the average density for the impact parameter taken into consideration.

2.5 Heavy-ion reaction

In recent years, the study of heavy ion induced reactions has been become a topic of interest in nuclear physics.Because of the heavy mass of the incident heavy ion, a lot of energy and angular momentum can be imparted to the target nucleus giving rise to new phenomenon, e.g fusion-fission, etc. Any Particles(projectiles)heavier than alpha (He^4) considered as heavy ions. So any ion from He^4 up to Pb^{208} or U^{238} is a heavy

ion.Reactions have been studied using a large number of heavy ions as projectiles. Very commonly used heavy ions are: Li^6, C^{12},N^{14}, O^{16}, Ne^{20}, Mg^{24}, Al^{27}, S^{32}, Ca^{40}, Cr^{52}, Ni^{58}, Sn^{120}, Pb^{208},etc.

The heavy ion induced reaction is somewhat complex because of the complexity of the incident projectile. The complex nature of the projectile makes it possible that a number of new reactions occur, and also when the projectile fuses with the target nucleus creating a compound nucleus one has to consider the special features of the heavy-ion reaction due to the large angular momentum carried in by the projectile.

At low energies two heavy ions interact only through their Coulomb fields, and can scatter elastically or inelastically with coulomb excitation. Nuclear reactions can only take place if the two-ion energy E_{cm} in their center of mass system is high enough to overcome the Coulomb barrier, and then the associated wave length $\lambda = h/\sqrt{2ME_{cm}}$ is much less than the nuclear dimensions. In such circumstances the interaction shows semiclassical features, and in particular it is appropriate to consider the ions moving along their classical orbits . This semiclassical nature of the heavy-ion interactions makes it possible to give an overall description in terms of the minimal distance between the two interacting ions r_{min} which is simply related to the impact parameter b by

$$r_{min} = \frac{b}{\sqrt{1 - \frac{V(r_{min})}{E_{CM}}}} \tag{2.5.1}$$

Where $V(r_{min})$ is the nuclear potential acting between the two ions. Even though such a description is only qualitative and a full treatment must take account of the quantum mechanical nature of the process, it is possible to distinguish four regions where the different reaction mechanism predominates as the minimal distance between the two ions increases:

(1)the fusion or compound nucleus formation region, with $0 \leq r_{min} \leq R_F$;

(2)the deep inelastic and the incomplete fusion region with $R_F < r_{min} \leq R_{DIC}$;

(3)the grazing region with $R_{DIC} < r_{min} \leq R_N$;

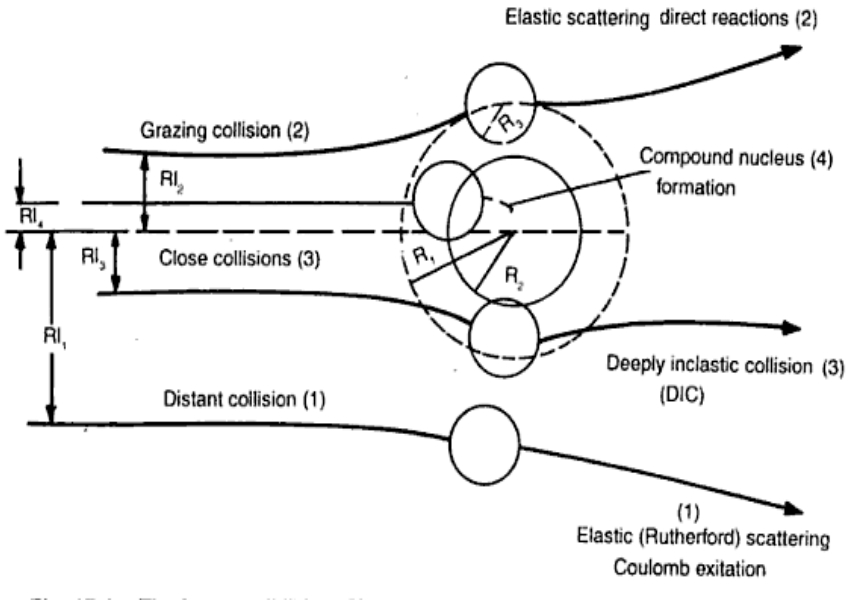

Figure 2.7: The four possibilities of heavy ion interactions, as seen classically showing the trajectories, corresponding to distant collision (Trajectory1), grazing (Trajectory2), close collisions (Trajectory3), and for compound nucleus formation (Trajectory4).

(4) the Coulomb region with $r_{min}>R_N$, where R_N is the distance above which nuclear interactions are negligible.

The ion orbits corresponding to these regions are schematically shown in fig.2.7. Nuclear reactions, induced by heavy ions below but near Coulomb barrier are useful for exciting the collective model of excitation of the target nuclei.

Because Coulomb barrier is comparatively high in heavy ion-induced reactions and the projectile energies generally available are of the same order as the Coulomb barrier, the Coulomb barrier energy becomes very good reference energy to describe the reactions. Further, one can decide the reactions according to the impact parameter (R_1) in a semi classical manner. It may be noted, that the impact parameter is the closest distance of approach of the projectile as indicated in fig 2.7.

One, then,has the following possibilities:

i)If $R1_1>>R = R_1 + R_2$, the projectile passes quite away from the nuclear range of interaction of the two nuclei and only Coulomb interaction is possible between the projectile

and the target. Then only Rutherford elastic scattering takes place, or the target and/or projectile may be internally excited, through Coulomb excitation giving rise to inelastic scattering of the projectile. This is shown in trajectory (1) in fig 2.7.

ii)If $R1_2 is \approx R_1 + R_2$, i.e. the outer surface of the incident projectile just grazes along the surface of the target nucleus, then the edges of the nuclear ranges of the nuclei just touch, so that only the outer portions of the skins of the two nuclei interact. Then only the extremely outer lying nucleus in the two nuclei comes within the nuclear range of interaction. This may, lead to one or two nucleon-transfer from one nucleus to the other or only elastic scattering or inelastic scattering may take place when any one of the two nuclei are internally excited, either via Coulomb excitation or nuclear interaction. This is induced by trajectory (2) in fig 2.7.

iii)If $R1_3 \leq R_1 + R_2$, i.e. the incident projectile just enters the nuclear range of the interaction of the two nuclei. This is a case, where nuclear interaction is prominent and elastic scattering is nearly absent. Then deep inelastic collisions predominate. Here a few nucleons from one to five or six nucleons can get transferred from one nucleus to the other.

iv)If $R1_4 << R_1 + R_2$ and the energy of the incident projectile is high enough, so that it can penetrate the Coulomb barrier, the projectile, then enters the nuclear body much beyond the nuclear skin. Then the interaction of the nucleons in the incident nucleus will be very strong with the nucleus in the target nucleus giving rise to various phenomena, e.g

(1) fusion: so that the two nuclei completely merge into each other giving rise to the highly excited state of the compound nucleus, which decays through gamma emission.

(2) fusion-neutron Evaporation: In this case, the compound nucleus may decay to another nuclear species, by the evaporation of many neutrons from the compound nucleus. This may lead to exotic nuclei.

(3) fusion-fission: so that after the compound nucleus formation, it fission into two less

heavy nuclei-according to laws of fission.

As the projectile is heavy and target nucleus also heavy, therefore there is involvement of large mass (large number of nuclei) in nuclear reaction. As a result, in nuclear reactions induced by heavy ions:

(a)There may be transfer of huge mass or large number of nucleons. From a single nucleon transfer to large number of nucleon transfer may take place.

(b)Transfer of very large energy and momentum takes place. In these reactions we get highly excited states with large angular momentum transfer.

(c)We can also populate nuclei which are far away from the stability line. Such nuclei which either have large number of neutrons or protons (not available in nature) can be produced which are called Exotic nuclei.

(d)Due to large amount of mass transfer and also in the decay (after reaction) we may have emission of several types of systems, i.e. light particles, nucleons and also heavy elements (heavy fragments). The measurement of decay products is not an easy task. It involves certain special types of detecting or analyzing systems.

It has observed that at energies just above the coulomb barrier, the dominant reaction mechanism in heavy ion reactions are complete and incomplete fusion.

2.5.1 Complete Fusion Of Heavy Ion

In the Complete Fusion reactions is the process in which the projectile completely fuses with the target, which leads to the formation of excited composite system. And then it de-excites by particle and/or gamma-ray emission.Heavy ion complete fusion reaction is a reaction where there is an entire momentum transfer from projectile to the target nucleus take place.In this reaction,a fully equilibrated excited compound nucleus of pre-determined charge,mass and angular momentum is formed.

If the heavy ion is having sufficent energy to over come the potential barrier the chance

of its complete fusion increases. Also the complete fusion depends up on the impact parameter when b< R_{ion} + R_{nuc} and energy is a round or more than coulomb barrier,the complete fusion of projectile may take place and the formation of compound nucleus is possible.

This complete fusion reaction of heavy ion will be more at at high energy as compare with incomplete fusion.also the chance of pre-equilibrum decay of compoud system(before the statistical equilibrume is established) are more at the high energy.so complete fusion,Incomplete fusion and pre-equilibrum decay theories can be tested using various energies projectile.

When the impact parametere is on the order of b≈ R_{nuc} , It is possible to have in-elastic scattering or direct reaction(interaction of projectile with few nucleons). These are also deep in-elastic collistion which are slightly slower than the direct reaction.

2.5.2 Incomplete Fusion Of Heavy Ion

In the case of Incomplete Fusion reactions mechanism, the projectile breaks into two fragments, of which one will fuse with the target to form an excited composite system, which may decay via emission of light-particles and/or gamma-rays, while the other fragment moves forward as spectator with same velocity as that of the projectile carrying a large part of the angular momentum and kinetic energy of the projectile.

Heavy ion indused reaction depend up on the energy of the projectile and also the value of impact parameter.

For larger impact parameter that means b> $R_{nuc} + R_{ion}$ the incident heavy ion will have interaction of the type of Elastic Scattering and coulomb excitation of nucleus which no nuclear force are involved.The nucleus is de-excited by the emission of photons or low energy $\gamma-$ ray.

As the impact parameter decreases that means b≈ $R_{ion} + R_{nuc}$ it is grazing incidence and

if the energy of heavy ion is small such that E< $\frac{Z_{ion}Z_{nuc}e^2}{4\pi\epsilon(R_{ion}+R_{nuc})}$ energy of heavy ion is below the coulomb barrier. then it is possible that there may be aparticle transfer of a nucleon from heavy ion.there may be small energy momentum transfer and few nucleon transfer this is also called Incomplete fusion of projectile.

From the projectile having $\alpha-$ type sturacture it is possible that only one $\alpha-$ particle is fused(enter). If the projectile is say $^{16}O(^{12}C+\alpha)$ from ^{16}O it is possible that only α is fused and ^{12}C is emitted out.

If the energy of the projectile is large enough,it is possible that in the coulomb field the projectile breaks and ^{12}C is fused while α is emitted.Incomplete fusion type reaction are possible for several projectile having $\alpha-$ type stracture. It is difficulte to predict Theoretically whether the $\alpha-$ particles emitted are before fusion or after the entering of projectile inside the nucleus.

Suppose ^{16}O is projectile out of thus ^{12}C is fused and α is emitted ^{12}C also inside breaks in to ^{8}Be and α so this α is also emitted.Therefore $\alpha-$ emitted out side(when HI is ^{16}O).Incomplete fusion of projectile will certanily depend up on the energy of projectile.

Chapter 3

EXPERIMENTAL DETAILS AND COMPUTER CODES

3.1 Experimental Method

Since this is very costy, it will not be easy to get either the well equipped Expermental laboratory or the access for conducting this experiment here in Ethiopia.Therefore the experment results were taken from the measurement done at the in India.

In these experment stacks were consisted by two self-supporting targets of 1.1 mg/cm^2 niobium separated by 2 mg/cm^2 Aluminium foils.seven irradiation were carried out for each such stack of target and degraders to encompass the 16-O beam energy between 70 and 100 MeV.

This chamber has a facility of in vacuum transfer of targets,which minimizes the time-lapes between the stopping of irradiation and the beginning of counting. A typical stacked foil arrangement used for excitation function measurements is shown in figure below.

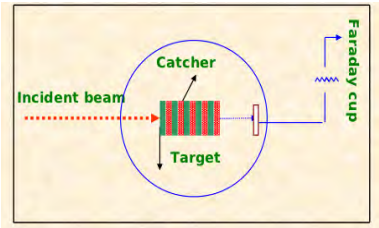

Figure 3.1: A typical experimental set up for the measurement of EFs

The irradiation of the stack covered the desired energy range of ≈ 70-100 MeV in measuring the EFs of various evaporation residues produced in the $^{16}O + ^{93}Nb$ system. To ensure more efficent collection of CF and ICF products,the thickness of Al backings was carefully chosen. The irradiation times were selected according to the half-lives of the radioioisotopes produced. Electero-suppressed Faraday cup was placed behind the target assembly.

Expermentally,the cross-section σ_r(E) at a given energy E for different reactions was determined using the expression as,

$$\sigma_r(E) = \frac{c\lambda e^{\lambda t_1}}{N_o \xi \varphi \theta G_e (1 - e^{-\lambda t_i})(1 - e^{-\lambda t})} \tag{3.1.1}$$

where cλ is activity of the isotope produced in t_i,φ is the incident flux, θ is the branching ratio of identified γ - ray and G_e is the geometry dependent efficiency of the detector for particular energy E.

The quantity ξ is the correction for self absorption of the γ-ray with absorption coefficent μ for the sample of thickness d,and it is given as

$$\xi = \frac{(1 - e^{-\mu d})}{\mu d} \tag{3.1.2}$$

The errors in the measured production cross-section may arise mainly because of

(1)The non-uniform thickness of samples that may lead to the uncertainty in the determination of the number of target nucli and is estimated to be 5-8 percent.

(2)Fluctuation in the beam current may result in the variation of incident flux, proper

care were taken to keep the beam current constant as far as possible and it is estimated to be less than 5 percent.

(3)The counting statistics 1-4 percent.

(4)The detection efficiency 4 percent.

(5)The gamma-ray intensity values 5-10 percent.These errors excluded uncertainity of the nuclear data such as branching ratio,decay constant etc.,which have been taken from tabel of isotopes. Attempts were made to minimize the uncertaninties caused by all the above possible factors.The Overall error in the present work is estimated to be less than or equal to 28 percent.

3.2 Computer Code Pace4

There are different computer codes to calculate the theoretical excitation functions. These are PACE4, CASCADE, ALIC-91 and COMPLET codes etc.

But in these thesis i used PACE4 to compare the experimental and theoretical value of excitation functions. because the pace4 code is based on a statistical approach.In this Program the de-excitaion of the compound nucleus is followed by a Monte-Carlo Procedure. The angular momentem projections are calculated at each stage of de-excitation, which enabels the de-excitation of the angular distribution of the emitted particles. and Here the level density Parameter is an important parameter which may be varied to match the experimental data. The Level density parameter obtained by experiment shows a linear dependent with the mass number of the compound nucleus. In general it is given by an expression,

$$a = \frac{ACN}{K} \tag{3.2.1}$$

Where 'ACN' is the mass of the compound nucleus and 'K' is the free constant.

Chapter 4

EXPERIMENTAL RESULTS AND ANALYSIS

In the present work the excitation functions for residues produced in the $^{16}O+^{93}Nb$ systems via CF and/or ICF processes were studied at projectile energies up to 100 MeV. To investigate those reaction dynamics,the excitation function for ^{106}In,^{105}In,^{105}Cd,^{104}Cd, ^{105}Ag, ^{104}Ag,^{103}Ag,^{102}Ag,^{101}Ag,^{101}Pd,^{100}Pd,^{100}Rh,^{99}Rh,^{98}Rh and ^{96}Tc radionuclide produced in this energy range were considered. The cross sections from a given reaction channel were determined separately from the observed intensities of all possible identified γ rays,arising from the same radionuclide. The reported values are the weighted average of the various cross-section values obtained[15] .An analysis of experimentally measured excitation functions was made using the theoretical prediction of the PACE4 code,which is developed based on statistical Hauser Feshback formalism followed by Monte Carlo simulation to determine the decay sequence of an excited compound nucleus.

This formalism takes angular momenteum directly in to account.The angular momentum projection are calculated at each stage deexcitation, which enebles the determination of the angular distribution of emited particles. The measured excitation functions were compared with the theoretical predictions obtained from the code PACE4. The Experimental cross-section is obtained from IAEA data source , (A.Sharma,B.B.Kumar,S.Mukherjee,S.chakrab ,S.B.Manohar) JOURN:JOUR.OF PHYSICS,PART G(NUCL.AND PART.PHYS.).VOL.25,P.2289 (1999)UK [15]. The theoretical and experimental cross-sections are plotted against the

projectile energy are shown in figures 4.1 to 4.15. The projectile energy is measured in Mega electrovolt (MeV) and the cross-section are measured in millibarn(mb). The experimental data for the reaction $^{93}Nb(^{16}O, 3N)$, $^{93}Nb(^{16}O, 4N)$,$^{93}Nb(^{16}O, p3n)$,$^{93}Nb(^{16}O, p4n)$, $^{93}Nb(^{16}O, \alpha)$,$^{93}Nb(^{16}O, \alpha n)$,$^{93}Nb(^{16}O, \alpha 2n)$, $^{93}Nb(^{16}O, \alpha 3n)$,$^{93}Nb(^{16}O, \alpha 4n)$,$^{93}Nb(^{16}O, \alpha p3n)$, $^{93}Nb(^{16}O, \alpha p4n)$,$^{93}Nb(^{16}O, 2\alpha n)$,$^{93}Nb(^{16}O, 2\alpha 2n)$, $^{93}Nb(^{16}O, 2\alpha 3n)$,$^{93}Nb(^{16}O, 3\alpha n)$,is taken from the Author (A.Sharma,B.B.Kumar,S.Mukherjee,S.chakrabarty,B.S.Tomar,A.Goswami ,S.B.Manohar) JOURN:JOUR.OF PHYSICS,PART G(NUCL.AND PART.PHYS.).VOL.25,P.2289 (1999)UK [15]. Energy range selected from the data is same with theoretical. The cross-section of theoretical and experimental with the energy range are given in table 4.1 to 4.15. The various parameters are used for calculation of excitation function. However, the level density parameter is found to play an important role in the theoretical predictions. In this thesis theoretical calculation is performed by the level density parameters $a = \frac{ACN}{8}$,$a = \frac{ACN}{10}$ and $a = \frac{ACN}{12}$.

4.1 The production of Indium ^{106}In

In the $^{93}Nb(^{16}O, 3n)^{106}In$ reaction,theoretically obtained results using pace4 are in good agreement with the expermentally measured data.so in this reaction the projectile is assumed to fuse completely with the target nucleus forming the excited state $^{109}In^{*}$,and this exited state emits three neutros during the thermalization, leaving behind the residual nucleus ^{106}In.for this reaction the complete fusion reaction are more dominante.

Table 4.1: Theoretical and Measured cross-section for the reaction $^{93}Nb(^{16}O, 3n)^{106}In$

$E - Lab$	$\sigma(Exp)$	Err	$\sigma(k = 8)$	$\sigma(k = 10)$	$\sigma(k = 12)$
70	78	9	72.8	97.1	110
75	45	11	45.6	54.8	44.4
80	38	11	30.6	38.4	39.5
85	16.8	11	5.31	11.9	17.3
90	3.5	11	0.761	4.08	4.62
95	0.97	12	0.114	0.855	1.03

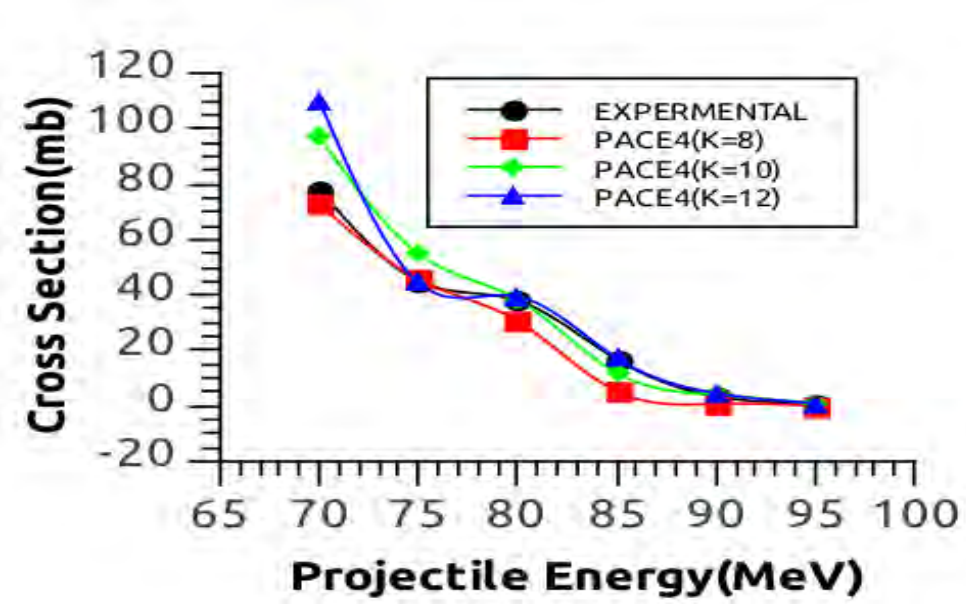

Figure 4.1: Theoretical and Measured cross-section for the reaction $^{93}Nb(^{16}O, 3n)^{106}In$

4.2 The production of Indium ^{105}In

In the $^{93}Nb(^{16}O, 4n)^{105}In$ reaction,In this reaction also theoretically obtained results using pace4 are comparable to the expermentally measured data.so in this reaction the projectile is assumed to fuse completely with the target nucleus forming the excited state $^{109}In^{*}$,and this exited state emits four neutrons during the thermalizatio, leaving behind the residual nucleus ^{105}In.for this reaction also the complete fusion reaction are more dominante.

Table 4.2: Theoretical and Measured cross-section for the reaction $^{93}Nb(^{16}O, 4n)^{105}In$

$E - Lab$	$\sigma(Exp)$	Err	$\sigma(k = 8)$	$\sigma(k = 10)$	$\sigma(k = 12)$
70	25	12	31.8	29.1	28.2
75	24.6	11	39.1	33.9	29.1
80	31	13	41.4	38.1	34.6
85	26	12	37.1	33.8	29.1
90	26	12	36.1	34.1	30.7
95	16	13	25.5	23.1	18.6
100	9.6	13	19.6	13.1	8.8

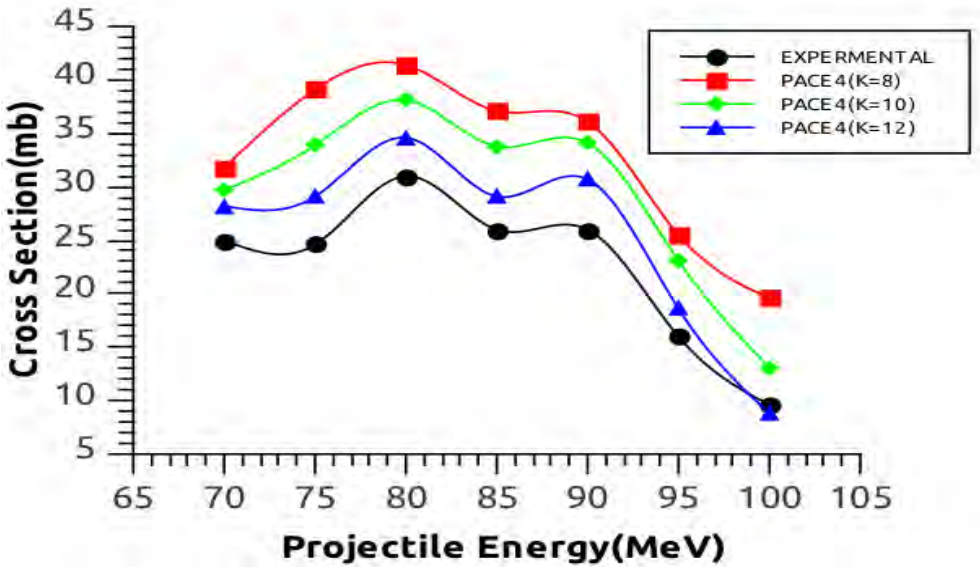

Figure 4.2: Theoretical and Measured cross-section for the reaction $^{93}Nb(^{16}O, 4n)^{105}In$

4.3 The production of Cadmium^{105}Cd

For the $^{93}Nb(^{16}O, p3n)^{105}Cd$ reaction,as shown in figure the theoretical caculation are almost comparable at higher energies with expermental data. from this observation,it is possible to explain this reaction as the complete fusion of the projectile with target.The reaction forms the excited state $^{109}In^{*}$,where this exited state emits one proton and three neutrons leaving behind the residual nucleus ^{105}Cd. It can be seen from this figure that the experimentally measured excitation function comparable with theoretical calculation particularly for free constant level density parameters at k=10 and k=12. as such it may be possible to say in this reaction the contribution coming from complete fusion is more dominant.

Table 4.3: Theoretical and Measured cross-section for the reaction $^{93}Nb(^{16}O, p3n)^{105}Cd$

$E-Lab$	$\sigma(Exp)$	Err	$\sigma(k=8)$	$\sigma(k=10)$	$\sigma(k=12)$
70	108	13	202	118	120
75	136	10	329	292	141
80	196	12	276	297	126
85	152	11	165	191	111
90	168	11	121	153	169
95	78	13	47.5	76.8	96.3
100	63	11	37.9	44.2	75.8

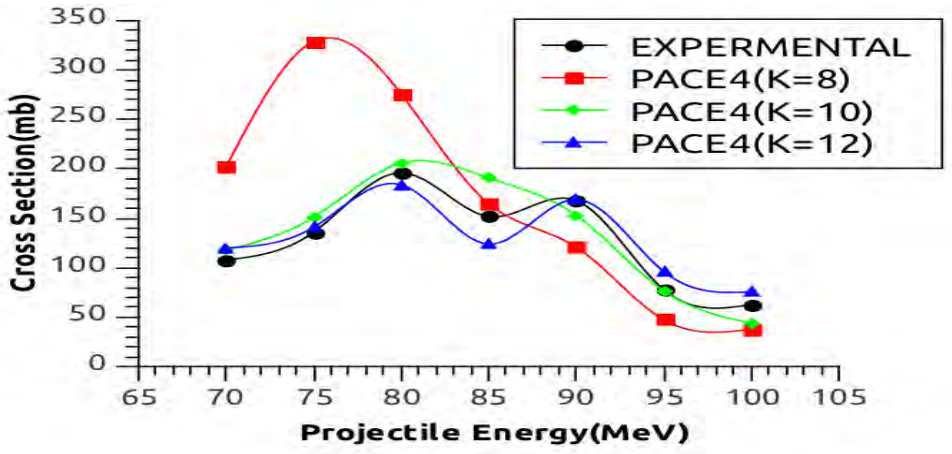

Figure 4.3: Theoretical and Measured cross-section for the reaction $^{93}Nb(^{16}O, p3n)^{105}Cd$

4.4 The production of Cadmium^{104}Cd

For the $^{93}Nb(^{16}O, p4n)^{104}Cd$ reaction,as shown in figure the theoretical caculation obtained results are almost comparable at lower energies with expermental data especially for k=12. here also from this observation,it is possible to explain this reaction as the complete fusion of the projectile with target.The reaction forms the excited state $^{109}In^*$,where this exited state emits one proton and four neutrons leaving behind the residual nucleus ^{104}Cd.Again here also it can be seen from this figure that the experimentally measured excitation function is close to the calculated theoretical excitation function especially for free constant level density parameter at k=12. Therefore,here also the contribution coming from complete fusion is more dominant.

Table 4.4: Theoretical and Measured cross-section for the reaction $^{93}Nb(^{16}O, p4n)^{104}Cd$

$E - Lab$	$\sigma(Exp)$	Err	$\sigma(k = 8)$	$\sigma(k = 10)$	$\sigma(k = 12)$
75	9.7	11	9.32	7.15	0.386
80	43	12	45.3	41.7	61.2
85	74	9	133	90.4	82.5
90	135	12	368	376	128
95	126	12	416	344	258
100	127	9	152	161	101

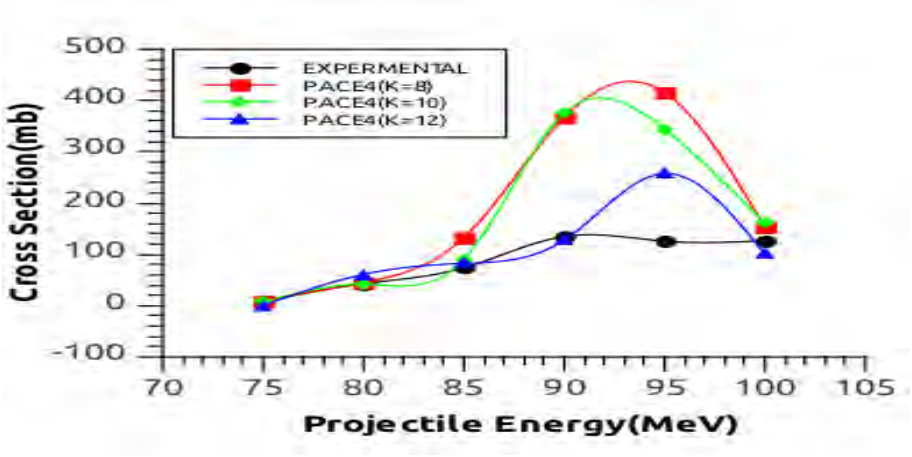

Figure 4.4: Theoretical and Measured cross-section for the reaction $^{93}Nb(^{16}O, p4n)^{104}Cd$

4.5 The production of Silver ^{105}Ag

For the $^{93}Nb(^{16}O, 2p2n)^{105}Ag$ reaction as shown in figure the theoretical calculated results using pace4 particularly for k=8 is in good agreement with the experimemtal measured excitation function.so complete fusion of the projectile with the target takes place. The production of ^{105}Ag leads to the sequential decay of two protons and two neutrons which means alpha particle in the de-excitation of the compound nucleus formed during the complete fusion of ^{16}O with ^{93}Nb. There is a negligible projectile ^{16}O break-up in to α and ^{12}C Therefor, complete fusion reaction is dominant and the small disagreement may be due to statistical uncertanities in the pace4 calculations.

Table 4.5: Theoretical and Measured cross-section for the reaction $^{93}Nb\ (^{16}O, 2p2n)^{105}Ag$

$E-Lab$	$\sigma(Exp)$	Err	$\sigma(k=8)$	$\sigma(k=10)$	$\sigma(k=12)$
70	21.3	5	23.6	29.7	29.1
75	40	13	51	54.8	54.8
80	69	10	77.1	113	90.5
85	70	11	91.3	133	110
90	87	13	97.4	114	138
95	72	11	74.5	88	97.4
100	57	11	45.9	42.7	68.2

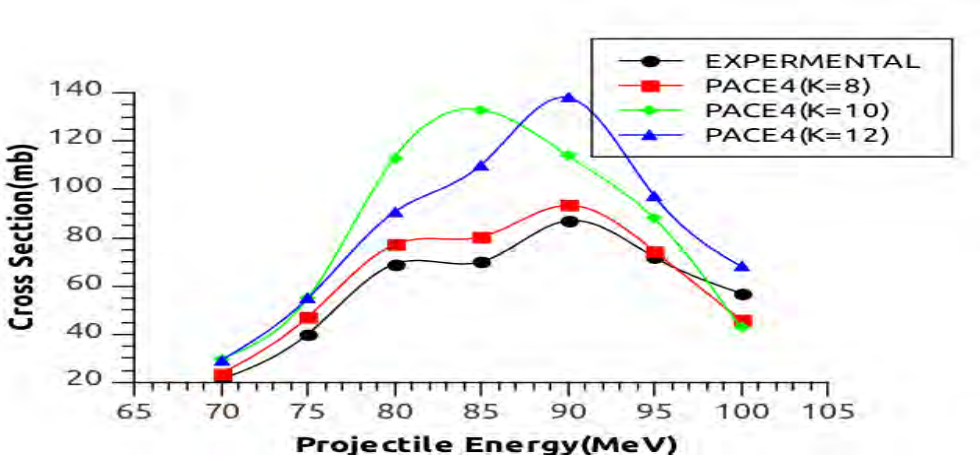

Figure 4.5: Theoretical and Measured cross-section for the reaction $^{93}Nb\ (^{16}O, 2p2n)^{105}Ag$

4.6 The production of Silver ^{104}Ag

For the $^{93}Nb(^{16}O, \alpha n)^{104}Ag$ reaction as shown in figure the theoretical calculated results using pace4 is slightly in good agreement with the experimemtal result at lower energies,where as the expermental result is larger than theoretical calculation at higher energies.This difference in the experimental and theoretical calculation may be due to the contribution coming from incomplete fusion. In this reaction it may be assumed that projectile(^{16}O) break-up in to α and ^{12}C . The ^{12}C fragment fuses with the target(^{93}Nb) forming the excited state $^{105}Ag^*$ while the rest fragment moves in the forward direction almost with the same velocity. The excited state $^{105}Ag^*$ may then emits one neutron then leaving behind the residual nucleus ^{104}Ag.

Table 4.6: Theoretical and Measured cross-section for the reaction $^{93}Nb\ (^{16}O, \alpha n)^{104}Ag$

$E - Lab$	$\sigma(Exp)$	Err	$\sigma(k=8)$	$\sigma(k=10)$	$\sigma(k=12)$
70	5.3	11	0.291	1.16	2.61
75	7	11	1.79	0.621	1.16
80	22.7	8	22.2	9.56	5.24
85	42	10	75.1	44.2	27.7
90	102	9	72.1	98.2	81.3
95	108	7	74.5	79.1	99.1
100	125	6	101	111	97.1

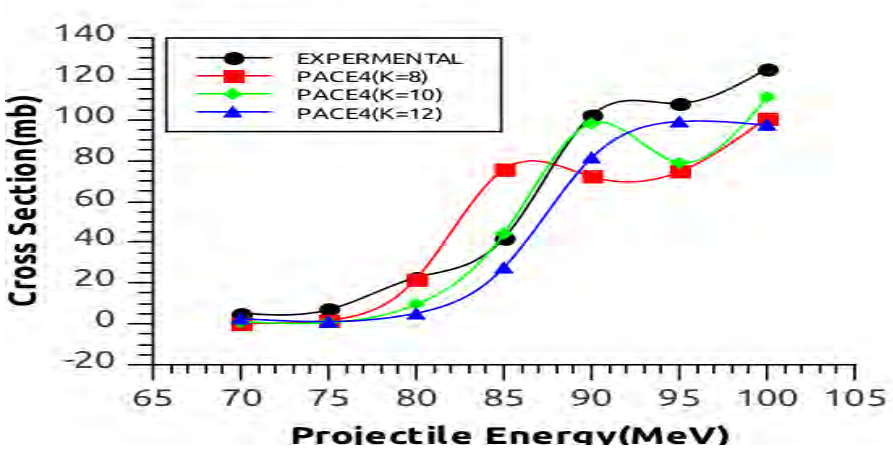

Figure 4.6: Theoretical and Measured cross-section for the reaction $^{93}Nb\ (^{16}O, \alpha n)^{104}Ag$

4.7 The production of Silver ^{103}Ag

For the $^{93}Nb(^{16}O, \alpha 2n)^{103}Ag$ reaction as shown in figure the theoretical calculated results using pace4 is slightly in good agreement with the experimemtal result at lower energies,where as the expermental result is larger than theoretical calculation at higher energies.This difference in the experimental and theoretical calculation may be due to the contribution coming from incomplete fusion. In this reaction it may be assumed that projectile(^{16}O) break-up in to α and ^{12}C . The ^{12}C fragment fuses with the target(^{93}Nb) forming the excited state $^{105}Ag^*$ while the rest fragment moves in the forward direction almost with the same velocity. The excited state $^{105}Ag^*$ may then emits two neutrons then leaving behind the residual nucleus ^{103}Ag.

Table 4.7: Theoretical and Measured cross-section for the reaction $^{93}Nb\ (^{16}O, \alpha 2n)^{103}Ag$

$E - Lab$	$\sigma(Exp)$	Err	$\sigma(k=8)$	$\sigma(k=10)$	$\sigma(k=12)$
70	70	9	73.6	75.8	78.8
75	59	12	54.8	58.8	54.8
80	62	8	64.3	49.9	67.2
85	40	10	28.9	33.3	33.3
90	45	11	13.2	19.2	16
95	46	11	28.8	21.2	24.8
100	49	10	25.2	38.1	37.9

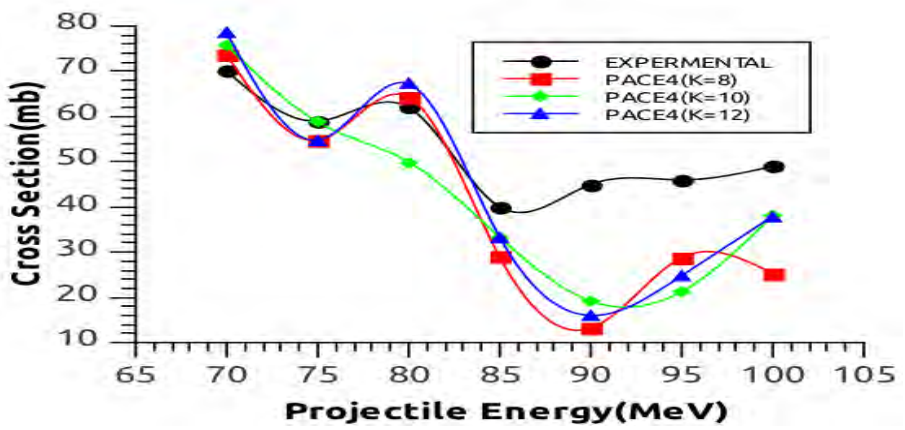

Figure 4.7: Theoretical and Measured cross-section for the reaction $^{93}Nb\ (^{16}O, \alpha 2n)^{103}Ag$

4.8 The production of Silver ^{102}Ag

For the $^{93}Nb(^{16}O, \alpha 3n)^{102}Ag$ reaction as shown in figure expermental results are much higher than the theoretical calculated results using pace4 at different k values. In this reaction the disagreement beteewen the experimental and theoretical result can be resolved by assuming the projectile (^{16}O) break-up in to α and ^{12}C where ^{12}C fuses with the target nucleus forming the excited state $^{105}Ag^{*}$.The excited state $^{105}Ag^{*}$ then emits three neutrons(3n) leaving behind the residual nucleus ^{102}Ag. from this it may be concluded that the contribution coming from the incomplete fusion reaction are more dominante.

Table 4.8: Theoretical and Measured cross-section for the reaction $^{93}Nb\ (^{16}O, \alpha 3n)^{102}Ag$

$E-Lab$	$\sigma(Exp)$	Err	$\sigma(k=8)$	$\sigma(k=10)$	$\sigma(k=12)$
70	100	9	70.7	70.7	70.4
75	163	13	122	73.1	81
80	204	7	193	77.1	71
85	255	11	111	72.4	80.5
90	228	9	71.1	35.5	71.1
95	174	9	9.48	19.8	27.3

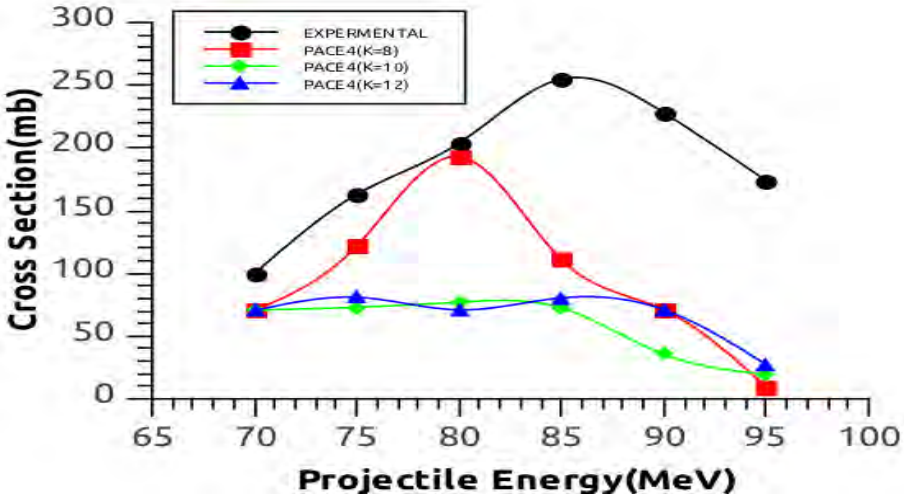

Figure 4.8: Theoretical and Measured cross-section for the reaction ^{93}Nb $(^{16}O, \alpha 3n)^{102}Ag$

4.9 The production of Silver ^{101}Ag

For the $^{93}Nb(^{16}O, \alpha 4n)^{101}Ag$ reaction as shown in figure the theoretical calculated results using pace4 is in good agreement with the experimemtal result at lower energies from 70-85 MeV ,where as the expermental result is lower than theoretical calculation at higher energies from 90-100 MeV. This difference in the experimental and theoretical calculation may be due to the contribution coming from incomplete fusion.In this reaction it may be assumed that projectile(^{16}O) break-up in to α and ^{12}C . The ^{12}C fragment fuses with the target(^{93}Nb) forming the excited state $^{105}Ag^*$ while the rest fragment moves in the forward direction almost with the same velocity. The excited state $^{105}Ag^*$ may then emits four neutron then leaving behind the residual nucleus ^{101}Ag.

Table 4.9: Theoretical and Measured cross-section for the reaction $^{93}Nb\ (^{16}O, \alpha 4n)^{101}Ag$

$E-Lab$	$\sigma(Exp)$	Err	$\sigma(k=8)$	$\sigma(k=10)$	$\sigma(k=12)$
70	3.89	8	0.186	0.126	0.105
75	6.3	8	0.311	0.311	0.155
80	9	10	7.5	10.8	2.44
85	13.4	7	12.9	17	21.3
90	25	8	32	64	96
95	28.8	7	129	134	127
100	32	9	133	150	183

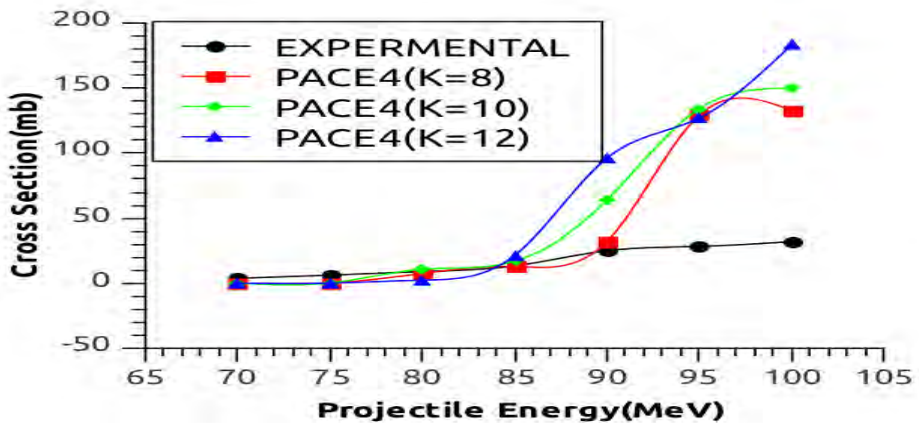

Figure 4.9: Theoretical and Measured cross-section for the reaction $^{93}Nb\ (^{16}O, \alpha 4n)^{101}Ag$

4.10 The production of Palladium ^{101}Pd

For the $^{93}Nb(^{16}O, \alpha p3n)^{101}Pd$ reaction as shown in figure the theoretical calculated results using pace4 are slightly closer to the expermental result,at lower energies.At higher energies there arises a disagreement between theoretical calculation and expermentally measured values, for this reaction, it is possible to assume the break-up of the projectile in to α and ^{12}C.The ^{12}C fuses with the target forming the excited state $^{105}Ag^{*}$, which emits one proton and three neutrons during thermalization and leaving behind the residual nucleus ^{101}Pd.so that the disagreement between the expermental and theoretical calculation could be infered to the contribution coming from the incomplete fusion reaction.

Table 4.10: Theoretical and Measured cross-section for the reaction $^{93}Nb\ (^{16}O, \alpha p3n)^{101}Pd$

$E-Lab$	$\sigma(Exp)$	Err	$\sigma(k=8)$	$\sigma(k=10)$	$\sigma(k=12)$
75	1.18	10	0.759	0.438	0.126
80	8.6	8	8.33	4.78	3.08
85	21.7	11	44.4	23.8	15.2
90	62	8	114	92.7	73.7
95	119	7	13.1	33.3	111
100	146	9	163	194	193

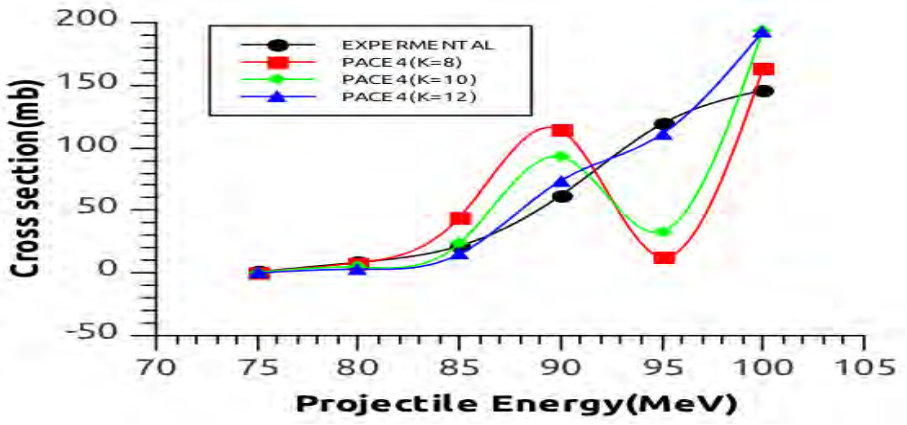

Figure 4.10: Theoretical and Measured cross-section for the reaction $^{93}Nb\ (^{16}O, \alpha p3n)^{101}Pd$

4.11 The production of Palladium ^{100}Pd

For the $^{93}Nb(^{16}O, \alpha p4n)^{100}Pd$ reaction also as shown in figure the theoretical calculated results using pace4 are slightly closer to the expermental result,at lower energies.At higher energies there arises a disagreement between theoretical calculation and expermentally measured values, for this reaction also it is possible to assume the break-up of the projectile in to α and ^{12}C.The ^{12}C fuses with the target forming the excited state $^{105}Ag^{*}$, which emits one proton and four neutrons during the thermalization and leaving behind the residual nucleus ^{100}Pd.so that the disagreement between the expermental and theoretical calculation could be infered to the contribution coming from the incomplete fusion reaction.

Table 4.11: Theoretical and Measured cross-section for the reaction $^{93}Nb\ (^{16}O, \alpha p4n)^{100}Pd$

$E-Lab$	$\sigma(Exp)$	Err	$\sigma(k=8)$	$\sigma(k=10)$	$\sigma(k=12)$
90	5.3	8	1.28	0.272	3.76
95	7.3	10	13.1	4.96	2.74
100	24.4	11	60	38.2	18.7

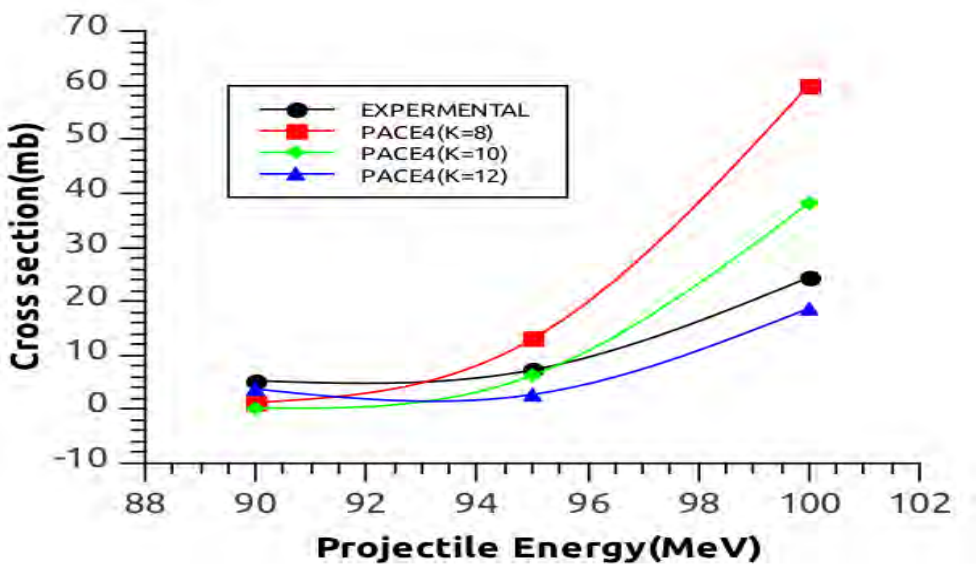

Figure 4.11: Theoretical and Measured cross-section for the reaction $^{93}Nb\ (^{16}O, \alpha p4n)^{100}Pd$

4.12 The production of Rhodium ^{100}Rh

For the $^{93}Nb(^{16}O, 2\alpha n)^{100}Rh$ reaction as shown in figure the theoretical calculated results using pace4 clearly shows a disagreement with the expermental measured values.Therefore,in this reaction it may be assumed that the projectile($16O$) break-up in to 2α and ^{8}Be.The ^{8}Be fragement fuses with the target($93Nb$) forming the excited state $^{101}Rh^{*}$,while the rest fragement moves in the forward direction almost with the same velocity.The excited state $^{101}Rh^{*}$ may then emits one neutron,during thermalization and leaving behind the residual nucleus ^{100}Rh.

Table 4.12: Theoretical and Measured cross-section for the reaction $^{93}Nb\ (^{16}O, 2\alpha n)^{100}Rh$

$E-Lab$	$\sigma(Exp)$	Err	$\sigma(k=8)$	$\sigma(k=10)$	$\sigma(k=12)$
70	5.7	9	6.19	12.7	16.5
75	8.8	11	4.5	10.3	18.2
80	9.2	15	1.62	6.63	14.7
85	9.6	10	0.997	2.72	8.97
90	9.3	11	0.631	1.68	3.99
95	8.3	8	1.32	1.01	1.82
100	12.3	10	5.82	4.82	2.91

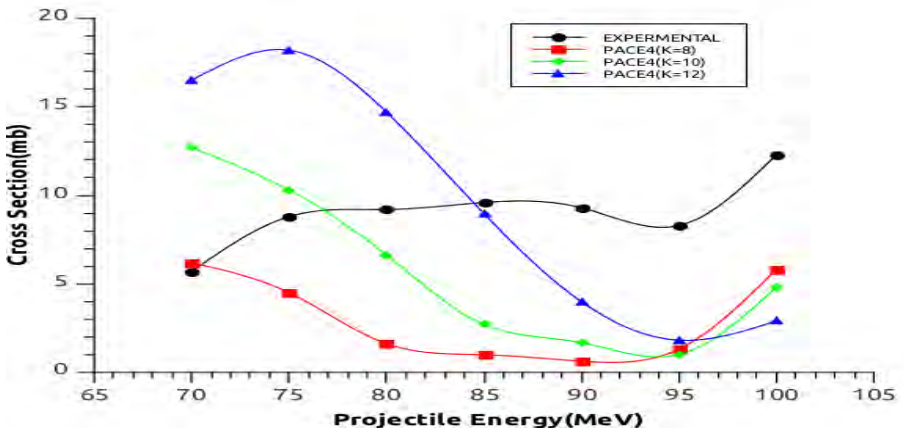

Figure 4.12: Theoretical and Measured cross-section for the reaction $^{93}Nb\ (^{16}O, 2\alpha n)^{100}Rh$

4.13 The production of Rhodium ^{99}Rh

For the $^{93}Nb(^{16}O, 2\alpha 2n)^{99}Rh$ reaction, as shown in figure the theoretical calculated results using pace4 are slightly closer to the expermental result,at lower energies particularly for k=8.At higher energies there arises a disagreement between theoretical calculation and expermentally measured values,as can be seen from the figure. for this reaction also it is possible to assume the break-up of the projectile in to 2α and ^{8}Be.The ^{8}Be fuses with the target forming the excited state $^{101}Rh^{*}$, which emits two neutrons during the thermalization and leaving behind the residual nucleus ^{99}Rh.so that the disagreement between the expermental and theoretical calculation could be infered to the contribution coming from the incomplete fusion reaction.

Table 4.13: Theoretical and Measured cross-section for the reaction $^{93}Nb\ (^{16}O, 2\alpha 2n)^{99}Rh$

$E-Lab$	$\sigma(Exp)$	Err	$\sigma(k=8)$	$\sigma(k=10)$	$\sigma(k=12)$
70	1.28	10	1.89	1.82	1.31
75	4.7	9	8.23	10.4	11.6
80	10.3	10	14.6	22.4	28.2
85	21	9	21.7	34.1	48.9
90	30.3	9	18.1	35.8	58.9
95	30.8	8	7.9	23.4	46.4
100	33.1	8	4.03	14.1	27.5

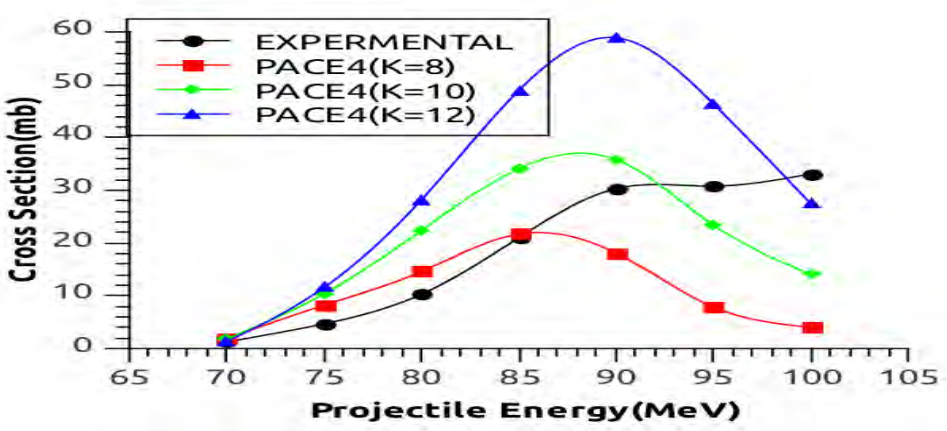

Figure 4.13: Theoretical and Measured cross-section for the reaction $^{93}Nb\ (^{16}O, 2\alpha 2n)^{99}Rh$

4.14 The production of Rhodium ^{98}Rh

For the $^{93}Nb(^{16}O, 2\alpha 3n)^{98}Rh$ reaction, as shown in figure the theoretical calculated results using pace4 are slightly closer to the expermental result,at lower energies.Again at higher energies there arises a disagreement between theoretical calculation and expermentally measured values,as can be seen from the figure. for this reaction also it is possible to assume the break-up of the projectile in to 2α and ^{8}Be.The ^{8}Be fuses with the target forming the excited state $^{101}Rh^{*}$, which emits three neutrons during the thermalization and leaving behind the residual nucleus ^{98}Rh.so that the disagreement between the expermental and theoretical calculation could be infered to the contribution coming from the incomplete fusion reaction.

Table 4.14: Theoretical and Measured cross-section for the reaction $^{93}Nb\ (^{16}O, 2\alpha 3n)^{98}Rh$

$E-Lab$	$\sigma(Exp)$	Err	$\sigma(k=8)$	$\sigma(k=10)$	$\sigma(k=12)$
80	0.65	12	0.386	0.308	0.0771
85	1.85	11	1.85	3.9	2.99
90	7.4	12	18.9	21.1	15.1
95	14.8	10	35.9	44	43.8
100	28	14	28.3	55.8	25.3

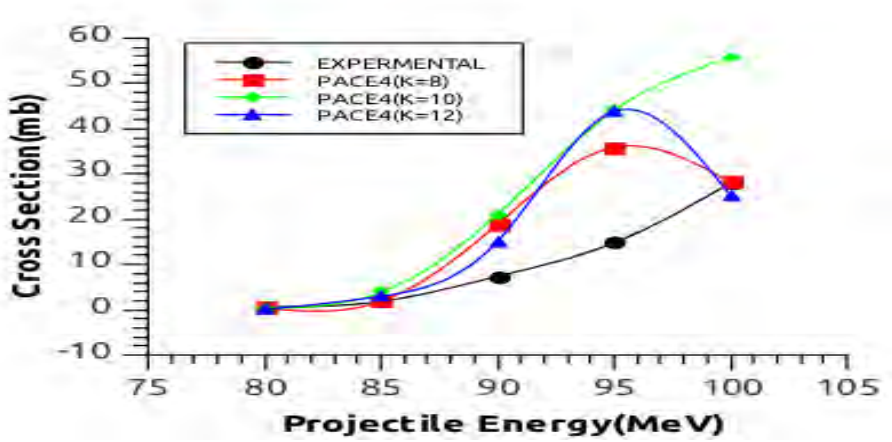

Figure 4.14: Theoretical and Measured cross-section for the reaction $^{93}Nb\ (^{16}O, 2\alpha 3n)^{98}Rh$

4.15 The production of Technetium ^{96}Tc

For the $^{93}Nb(^{16}O, 3\alpha n)^{96}Tc$ reaction as shown in figure it is clearly seen that the theoretically calculated cross section result using pace4 did not fit with the expermental cross section at all projectile energies.This may be due to the formation of incomplete fusion(ICF)reaction. For this reaction also assume the projectile(^{16}O) break up in to 3α and ^{4}He. The ^{4}He fragement fuses with the target (^{93}Nb) forming the excited state $^{97}Tc^{*}$ while the rest fragement moves in the forward direction almost with same velocity. the excited state $^{97}Tc^{*}$ may then emits one neutron , during thermalization and leaving behind the residual nucleus ^{96}Tc.

Table 4.15: Theoretical and Measured cross-section for the reaction $^{93}Nb\ (^{16}O, 3\alpha n)^{96}Tc$

$E-Lab$	$\sigma(Exp)$	Err	$\sigma(k=8)$	$\sigma(k=10)$	$\sigma(k=12)$
70	17.3	16	0.146	0.105	0.0728
75	23.2	9	0.621	0.155	0.155
80	25	12	0.593	0.893	1.08
85	26.5	10	0.72	1.18	0.181
90	31	13	1.47	3.15	3.99
95	31	13	1.01	3.24	5.77
100	30	17	0.336	2.46	5.94

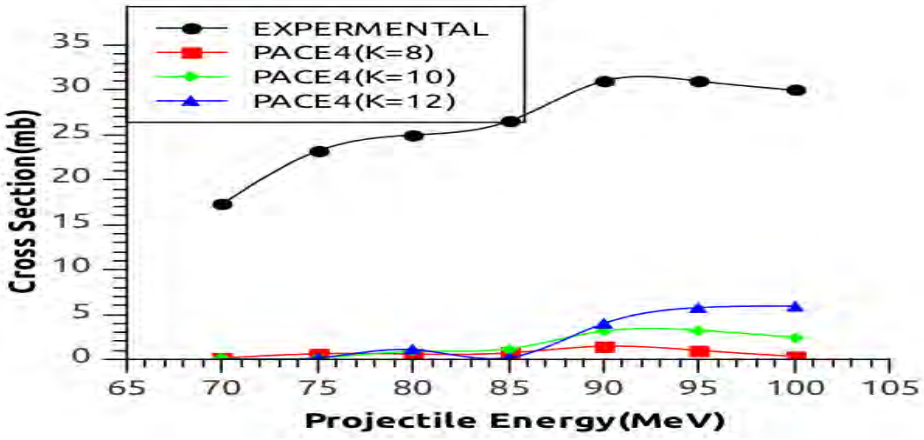

Figure 4.15: Theoretical and Measured cross-section for the reaction $^{93}Nb\ (^{16}O, 3\alpha n)^{96}Tc$

It is Possibel to Calculate the percent fraction of incomplete fusion (ICF) and its energy dependence for all α-emitting channels.

In the figure 4.16 the percentage of incomplete fusion in the formation of ^{102}Ag and ^{103}Ag are almost increasing through out its normalised energy ($E_{projectile}/V_{CB}$). In the case of formation of ^{104}Ag and ^{105}Ag when the projectile energy increasese the percentage of incomplete fusion formation decreases up to 85 mev.but at higher energy percentage of incomplete fusion formation of ^{104}Ag and ^{105}Ag are increasing.

Table 4.16: Calculation of percent fraction of incomplete fusion (ICF) and its energy dependence for α, αn,$\alpha 2n$,$\alpha 3n$ emitting channels respectively

E_{proj}/V_{CB}	$\frac{\sigma_{exp}-\sigma_{comp}}{\sigma_{exp}} \times 100$	$\frac{\sigma_{exp}-\sigma_{comp}}{\sigma_{exp}} \times 100$	$\frac{\sigma_{exp}-\sigma_{comp}}{\sigma_{exp}} \times 100$	$\frac{\sigma_{exp}-\sigma_{comp}}{\sigma_{exp}} \times 100$
1.6044	29.3	78.11	-8.285	-39.436
1.7190	55.153	91.128	0.338	-37
1.8336	62.2	57.885	19.516	-63.768
1.9482	71.607	-5.238	16.75	-90
2.0628	84.429	3.725	57.33	-31.0344
2.1774	94.55	26.759	53.914	-22.222
2.2920	-	11.2	22.245	25.0877

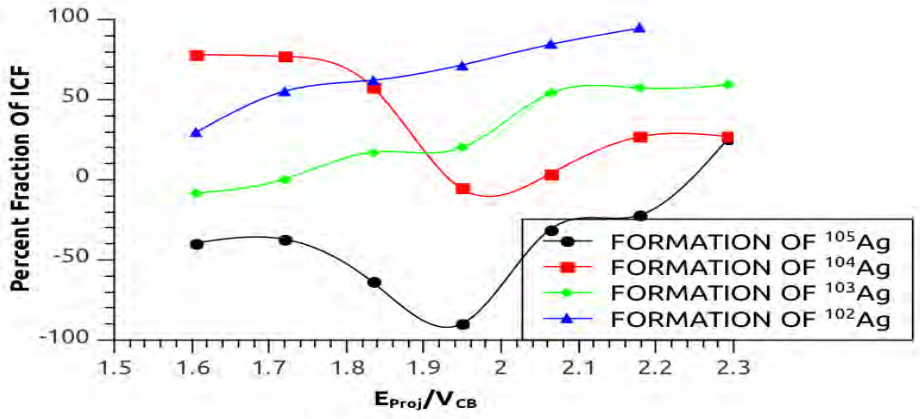

Figure 4.16: Calculation of percent fraction of incomplete fusion (ICF) and its energy dependence for α, αn,$\alpha 2n$,$\alpha 3n$

In the figure 4.17 the percentage of incomplete fusion in the formation of ^{101}Ag and ^{100}Pd when the projectile energy increasese the percentage of incomplete fusion formation decreases. So at lower energy high percentage of ^{101}Ag and ^{100}Pd are formed.here the breaking of projectile (^{16}O) is possible before entering the target nucleus due to columb force between projectile and target. In the case of formation of ^{101}Pd when the projectile energy increasese the percentage of incomplete fusion formation decreases up to 90 Mev but it increases up to 95 Mev and again it decreases up to 100 Mev. . For the formation of ^{100}Rh when the projectile energy increasese the percentage of incomplete fusion formation increases. So at higher energy high percentage of ^{100}Rh is formed. The breaking of projectile (^{16}O) is possible after entering the target nucleus due to columb force between

Table 4.17: Calculation of percent fraction of incomplete fusion (ICF) and its energy dependence for $\alpha 4n$,$\alpha p3n$,$\alpha p4n$,$2\alpha n$ emitting channels respectively

E_{proj}/V_{CB}	$\frac{\sigma_{exp}-\sigma_{comp}}{\sigma_{exp}} \times 100$	$\frac{\sigma_{exp}-\sigma_{comp}}{\sigma_{exp}} \times 100$	$\frac{\sigma_{exp}-\sigma_{comp}}{\sigma_{exp}} \times 100$	$\frac{\sigma_{exp}-\sigma_{comp}}{\sigma_{exp}} \times 100$
1.6044	95.141	-	-	-122.8
1.7190	95.06	62.88	-	-17.045
1.8336	-20	44.4186	-	27.935
1.9482	-26.865	-9.677	-	71.666
2.0628	-156	-49.516	94.867	81.935
2.1774	-365.277	72	32.054	87.832
2.2920	-368.75	-32.877	-56.558	60.814

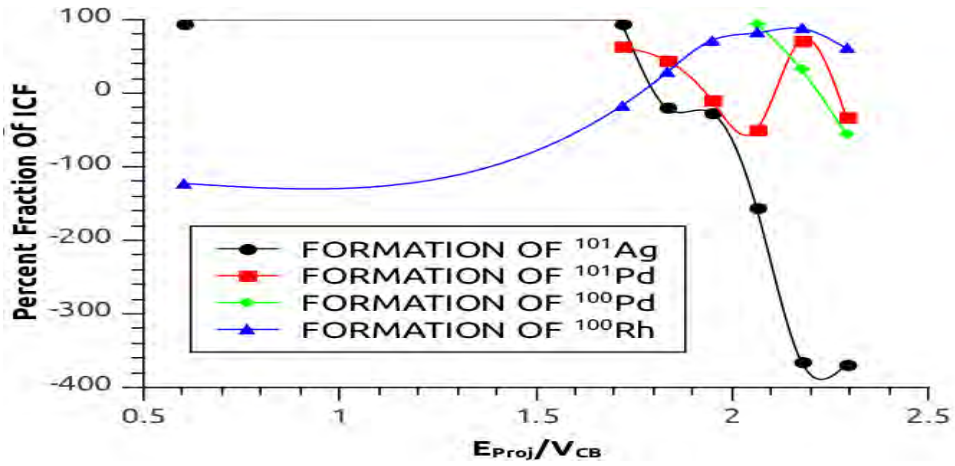

Figure 4.17: Calculation of percent fraction of incomplete fusion (ICF) and its energy dependence for $\alpha 4n$,$\alpha p3n$,$\alpha p4n$,$2\alpha n$

projectile and target is less. This may happen at the higher energies.

Table 4.18: Calculation of percent fraction of incomplete fusion (ICF) and its energy dependence for $2\alpha 2n$,$2\alpha 3n$,$3\alpha n$ emitting channels respectively

E_{proj}/V_{CB}	$\frac{\sigma_{exp}-\sigma_{comp}}{\sigma_{exp}} \times 100$	$\frac{\sigma_{exp}-\sigma_{comp}}{\sigma_{exp}} \times 100$	$\frac{\sigma_{exp}-\sigma_{comp}}{\sigma_{exp}} \times 100$
1.6044	-127.187	-	99.39
1.7190	-121.27	-	99.331
1.8336	-117.475	52.615	96.428
1.9482	-62.38	-110.810	95.548
2.0628	-18.152	-185.135	89.8387
2.1774	24	-197.298	89.549
2.2920	57.4	-99.285	91.8

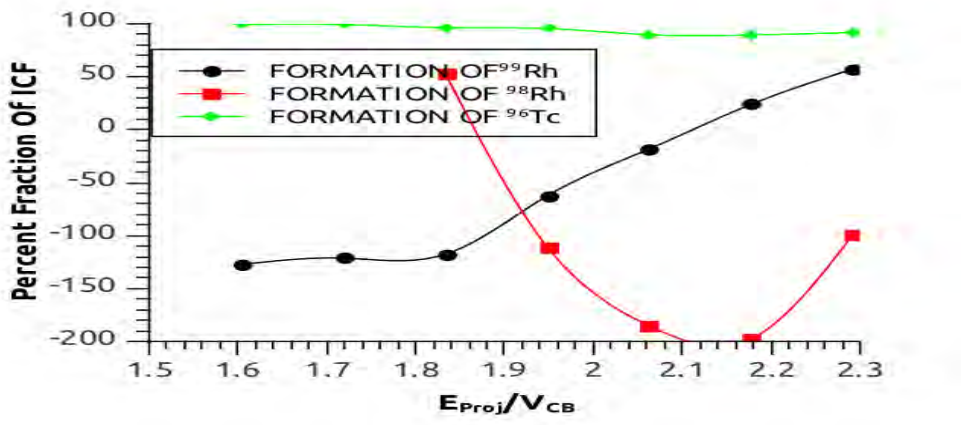

Figure 4.18: Calculation of percent fraction of incomplete fusion (ICF) and its energy dependence for $2\alpha 2n$, $2\alpha 3n$,$3\alpha n$

In the figure 4.18 the percentage of incomplete fusion fraction in the formation of ^{96}Tc is almost the same through out its normalised energy ($E_{projectile}/V_{CB}$). In the case of formation of ^{98}Rh when the projectile energy increasese the percentage of incomplete fusion formation decreases up to 95 Mev but at higher energy the percentage of incomplete fusion formation of ^{98}Rh increases. For the formation of ^{99}Rh when the projectile energy increasese the percentage of incomplete fusion formation increases. The break up is possible after the projectile enters the target.This may be at higher energy where the effect of columb repulsion is less.

Chapter 5

CONCLUSION

The Excitation functions for the (O,3n),(O,4n),(O,p3n),(O,p4n),(O,α),(O,αn), (O,α2n),(O,α3n) ,(O,α4n),(O,αP3n),(O,αP4n),(O,2αn), (O,2α2n),(O,2α3n) and (O,3αn) reactions for $^{16}O +^{93} Nb$ system have been studied in the energy range 70 - 100 MeV. The expermental data were compared with those calculated using the statistical de-excitation model code of PACE 4. For many case the expermental measured cross-section revealed agreement with PACE4 Calculation,especially in the lower energy region.

The experimentally studied production cross-sections for non-α emitting channels were found to be in good agreement with theoretical predictions which may be attributed to the complete fusion (CF) processes at these energies.

The residues ^{106}In , ^{105}In , ^{105}Cd and ^{104}Cd were formed by complete fusion (CF) from the excitation functions for the reactions $^{93}Nb(^{16}O, 3n)^{106}In$, $^{93}Nb(^{16}O, 4n)^{105}In$, $^{93}Nb(^{16}O, P3n)^{105}Cd$ and $^{93}Nb(^{16}O, p4n)^{104}Cd$ respectively . In the case of complete fusion (CF) the Projectile is completely fused with the target nucleus, leading to the formation of an excited composite system that may decay by the emission of n, p, etc., after attaining statistical equilibrium.

In case of α-emitting reactions, the experimental excitation functions exhibit a significant difference with theoretical Calculation in the production of cross-section, which may be attributed to the incomplete fusion (ICF) processes at these energies.

The residues ^{105}Ag , ^{104}Ag , ^{103}Ag,^{102}Ag,^{101}Ag,^{101}Pd,^{100}Pd,^{100}Rh,^{99}Rh, ^{98}Rh and ^{96}Tc

were formed by incomplete fusion (ICF) from the excitation functions for the reactions $^{93}Nb(^{16}O,\alpha)^{105}Ag$, $^{93}Nb(^{16}O,\alpha n)^{104}Ag$,$^{93}Nb(^{16}O,\alpha 2n)^{103}Ag$, $^{93}Nb(^{16}O,\alpha 3n)^{102}Ag$,$^{93}Nb(^{16}O,\alpha 4n)^{101}Ag$,$^{93}Nb(^{16}O,\alpha p3n)^{101}Pd$,$^{93}Nb(^{16}O,\alpha p4n)^{100}Pd$, $^{93}Nb(^{16}O,2\alpha n)^{100}Rh$,$^{93}Nb(^{16}O,2\alpha 2n)^{99}Rh$, $^{93}Nb(^{16}O,2\alpha 3n)^{98}Rh$ and $^{93}Nb(^{16}O,3\alpha n)^{96}Tc$ respectively . in the case of incomplete fusion (ICF) only a part of the projectile fuses with the target nucleus and the rest of it is going into the beam direction with almost the same velocity as that of incident ion beam. that means the projectile (^{16}O) breaks up into ^{12}C and an α-particle and ^{12}C fragment fuses with ^{93}Nb, forming the composite nucleus , followed by the emission of neutrons and α-particle.

Therefore from above analysis it may be conclude that in the case of complete fusion(CF) experimental and theoretical cross-sections are in good agreement while in the case of incomplete fusion experimental and theoretical cross-sections have large gap between them.

The measurment of energy spectrums of emitted α-particles,using inbeam experiments may tell the nature of breaking of projectile. That means the breaking of projectile ^{16}O is possible either before entering to the target nucleus,due to columb force between projectile and target.This may happen at the lower energies or it may be possible after the projectile enters to the target nucleus.This may be at higher energy where the effect of columb repulsion is less.

Bibliography

[1] B.S.Tomar et al, phys.Rev.c 49(1994)

[2] R. Ali et al. J. Phys. G: Nucl. Part. Phys. 37 (2010) 11510.

[3] H. C. Britt and A.R. Quinton, Phys. Rev. 124 (1961) 877.

[4] T.Inamura et al. Phys. Lett. B 68 (1977) 51

[5] T.Inamura,M.Ishihara,T. Fakuda, T.Shimoda,H.Hiruta,phys.Lett.B 68,51(1977)

[6] Unnati, p.p.Singh,D.P Singh,M.K. Sharma,A.Yadav,R.Kumara,B.P.Singh,and R Prased,Nucl.phys.A811,77(2008).

[7] E.A.Bakkum,P.Decowski,K.A.Griffioen,R.J.Meijer,and R.Kamermans,phys.Rev.c 39,2094(1989)

[8] J.H Barker et al,phys. Rev.Lett. 45,424(1980).

[9] T.Udagawa,T.Tamura,phys.Rev.Lett.45,1311(1980).

[10] J.Wilczynski,K.Siwek-Wilczynska,J.VanDriel,S.Gonggrijp,D.C.J.M.Hageman;R.V.F. Janssens, J.Lukasiak,R.H .Siemssen,S.Y.Van Der Werf,Nucl.phys.A373,109 (1982)

[11] M.Blann, phys.Rev.Lett.27,337(1971)

[12] R.Weiner et al.,Nucl.phys.A286,282(1980)

[13] J.P.Bondrof et al.,Nucl.phys.A333,285(1980)

[14] V.I Zagrebaev,Ann.phys.(NY)197,33(1990)

[15] (A.Sharma,B.B.Kumar,S.Mukherjee,S.chakrabarty,B.S.Tomar,A.Goswami,S.B.Manohar) JOURN:JOUR.OF PHYSICS,PART G(NUCL.AND PART.PHYS.).VOL.25,P.2289 (1999)UK.

[16] P.E.Hodgson,Nuclear reactions and nuclear structure(Clarendon,Oxford,1997)

[17] R.singh and S.N MukherJee,Nuclear reaction, New age international limited(1996)

[18] S.N.Goshoshal Atomic and nuclear Physics Vol-2,S.ChandCompany.New Delhi(1997)

[19] I.P.Jeremy and N.Sblomo,Modern physics:An introductory Text,Imperial College press(2000)

[20] J.M Blatt and V.F.Weisskopf,Theoretical nuclear physics (Wiley,New York,1952)

[21] R.singh and S.N MukherJee,Nuclear reaction, New age international limited(1996)

[22] J.J Griffin,Phys.Rev.Letts.17,478(1966)

[23] M.Blann,Phys.Rev.Letts.28,757(1972)

[24] A.Garvon,Phys.Rev.C21(1980)230

[25] EXFOR data source IAEA,Vienna(2004) or Exfor library:http:// www.nndc.bnl.gov/exfor.

[26] Investigation of the influence of incomplete fusion on the complete fusion on ^{12}C induced reactions at 4-7.2 MeV/nucleon F.K. Amanuel, B.Zelalem, A.K.Chaubey etal, the European physical Journal A-Hadrons and nucleus vol 47, Number 12,156(2011)

Declaration

This thesis is my original work, has not been presented for a degree in any other University and that all the sources of material used for the thesis have been dully acknowledged.

Name: Desalegn Ketema

Signature:

Place and time of submission: Addis Ababa University,June 2013

This thesis has been submitted for examination with my approval as University advisor.

Name: Prof.A.K.CHAUBEY

Signature: